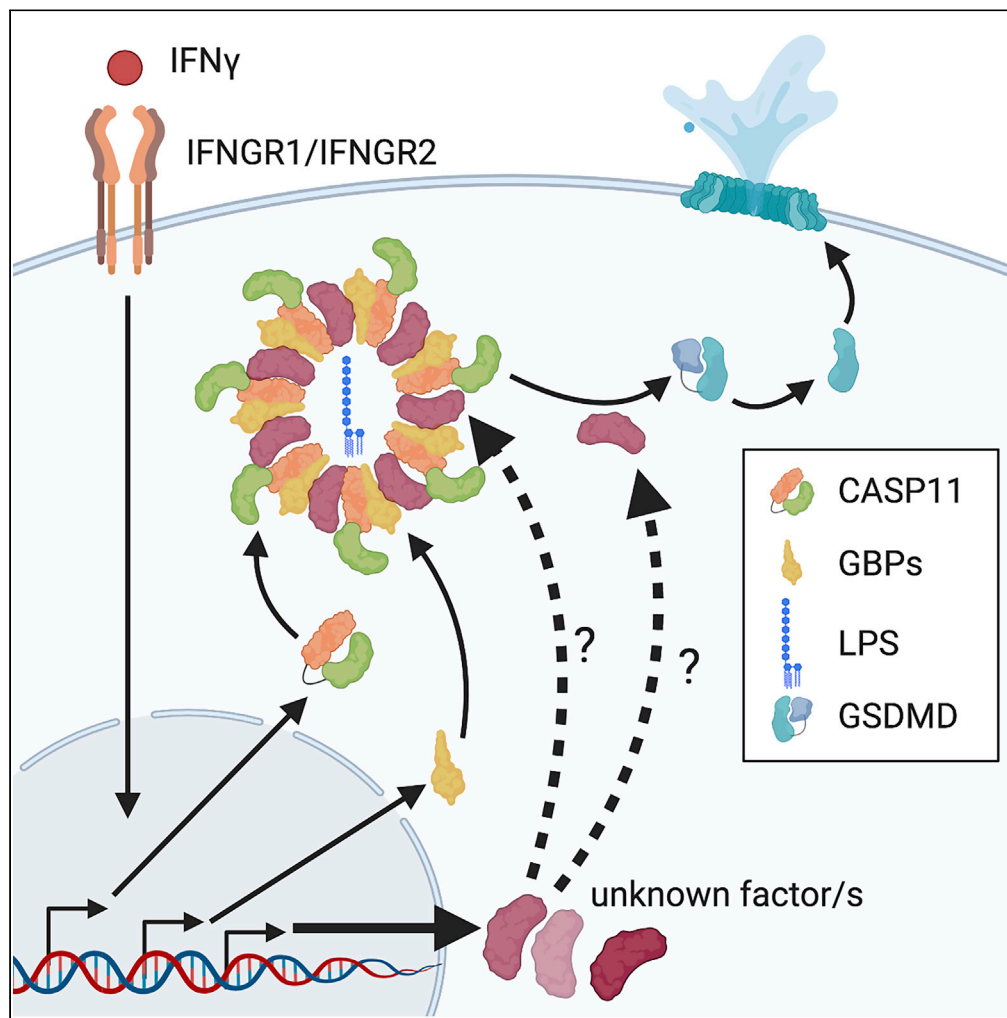


Article

# A Rapid Caspase-11 Response Induced by IFN $\gamma$ Priming Is Independent of Guanylate Binding Proteins



Sky W. Brubaker,  
Susan M. Brewer,  
Liliana M. Massis,  
Brooke A. Napier,  
Denise M. Monack

dmonack@stanford.edu

**HIGHLIGHTS**

IFN $\gamma$  priming elicits the most rapid and amplified response to cytosolic LPS

The enhanced IFN $\gamma$ -triggered response is separable from CASP11 expression

The enhanced IFN $\gamma$ -triggered response is independent of GBPs encoded on chromosome 3

We propose an unknown IFN $\gamma$ -induced regulator of CASP11-dependent pyroptosis exists

Brubaker et al., iScience 23, 101612  
October 23, 2020 © 2020 The Authors.  
<https://doi.org/10.1016/j.isci.2020.101612>



## Article

# A Rapid Caspase-11 Response Induced by IFN $\gamma$ Priming Is Independent of Guanylate Binding Proteins

Sky W. Brubaker,<sup>1</sup> Susan M. Brewer,<sup>1</sup> Liliana M. Massis,<sup>1</sup> Brooke A. Napier,<sup>2</sup> and Denise M. Monack<sup>1,3,\*</sup>

**SUMMARY**

**In mammalian cells, inflammatory caspases detect Gram-negative bacterial invasion by binding lipopolysaccharides (LPS). Murine caspase-11 binds cytosolic LPS, stimulates pyroptotic cell death, and drives sepsis pathogenesis. Extracellular priming factors enhance caspase-11-dependent pyroptosis. Herein we compare priming agents and demonstrate that IFN $\gamma$  priming elicits the most rapid and amplified macrophage response to cytosolic LPS. Previous studies indicate that IFN-induced expression of caspase-11 and guanylate binding proteins (GBPs) are causal events explaining the effects of priming on cytosolic LPS sensing. We demonstrate that these events cannot fully account for the increased response triggered by IFN $\gamma$  treatment. Indeed, IFN $\gamma$  priming elicits higher pyroptosis levels in response to cytosolic LPS when macrophages stably express caspase-11. In macrophages lacking GBPs encoded on chromosome 3, IFN $\gamma$  priming enhanced pyroptosis in response to cytosolic LPS as compared with other priming agents. These results suggest an unknown regulator of caspase-11-dependent pyroptosis exists, whose activity is upregulated by IFN $\gamma$ .**

**INTRODUCTION**

The innate immune response to lipopolysaccharide (LPS) at a cellular level is compartmentalized, allowing for distinct responses to Gram-negative pathogens based on subcellular localization (Brubaker et al., 2015). Extracellular LPS engages Toll-like receptor 4 (TLR4) at the plasma membrane and induces the transcription of pro-inflammatory cytokines such as IL-6, pro-IL-1 $\beta$ , pro-IL-18, as well as type-I interferons (IFN $\alpha/\beta$ ) (Akira and Takeda, 2004). In contrast, the response to cytosolic LPS triggers an inflammatory form of programmed cell death termed pyroptosis by binding to murine Caspase-11 (CASP11) or either human Caspase-4 or Caspase-5 (CASP4, CASP5) (Kayagaki et al., 2013; Hagar et al., 2013; Shi et al., 2014). These inflammatory caspases, as well as Caspase-1 (CASP1), are cysteine proteases that control pyroptosis by enzymatically cleaving gasdermin D (GSDMD) (Shi et al., 2015; Kayagaki et al., 2015). Following GSDMD cleavage, N-terminal "p30" GSDMD domain subunits (NT-GSDMD) oligomerize and form pores in the plasma membrane (Ding et al., 2016; Liu et al., 2016; Aglietti et al., 2016). These pores result in cell membrane damage and ultimately death. The response to cytosolic LPS is also associated with release of bioactive IL-18 and IL-1 $\beta$ , which requires active CASP1 for processing (Kayagaki et al., 2011). Mechanistically CASP1 is activated downstream of CASP11 through NLRP3-dependent sensing of K<sup>+</sup> efflux that results from NT-GSDMD pore formation (Ruhl and Broz, 2015).

Increasingly, evidence supports the idea that the macrophage response to cytosolic LPS is regulated by extracellular stimuli. For example, members of the IFN family of cytokines influence the macrophage response to cytosolic LPS. Several reports indicate that IFNs upregulate the expression of CASP11, which is believed to increase sensitivity to cytosolic LPS by facilitating the chance of interaction (Rathinam et al., 2012; Broz et al., 2012; Meunier et al., 2014). Indeed, a set of TLRs trigger the production of IFN $\alpha/\beta$  and thus TLR ligands are commonly used to enhance the macrophage response to cytosolic LPS. Additionally IFNs promote the expression of a set of GTPases known as the guanylate binding proteins (GBPs), which are recruited to microbe-associated membranes including endosomes, pathogen-containing vacuoles, as well as microbial membranes (Tretina et al., 2019). At these sites, and in the context of Gram-negative bacterial infections, murine GBPs encoded on chromosome 3 facilitate CASP11/4/5-dependent responses to LPS (Meunier et al., 2014; Pilla et al., 2014; Finethy et al., 2015). Recent studies in human cells have further

<sup>1</sup>Department of Microbiology and Immunology, Stanford University School of Medicine, Stanford, CA 94305, USA

<sup>2</sup>Biology Department, Portland State University, Portland, OR 97201, USA

<sup>3</sup>Lead Contact

\*Correspondence: dmonack@stanford.edu  
<https://doi.org/10.1016/j.isci.2020.101612>



elucidated the role of GBPs in this process by providing evidence that a GBP signaling platform is assembled with LPS to facilitate CASP4 activation (Wandel et al., 2020; Santos et al., 2020). Both studies provide evidence that human GBP1 is critically required for assembling a complex with LPS, GBP2, GBP3, GBP4, and CASP4 for inflammasome activation. Thus, IFNs promote the transcriptional upregulation of factors that enhance pyroptosis in response to LPS in the cytosol.

Despite many insights into the transcriptional control of pyroptosis regulators by these extracellular signals, the functional differences between IFNs and TLR ligands when comparing inflammasome activation remains poorly defined. One reason for this lack of clarity derives from the fact that many studies have examined the distinct activities of IFNs or TLR ligands individually on the effects of pyroptosis. These events are hereafter referred to as “priming” events and represent activities that increase the rate or magnitude of pyroptosis. In this study, we compared the effects of IFN or TLR4 priming on CASP11 inflammasome activation to characterize differences in how these extracellular stimuli regulate the response to cytosolic LPS.

We demonstrate that type II IFN (IFN $\gamma$ ), as compared with IFN $\beta$  or LPS, is the most potent at enhancing CASP11-dependent pyroptosis induced by cytosolic LPS in murine macrophages. This enhancement may be relevant during infection with Gram-negative bacteria given that IFN $\gamma$  production *in vivo* is critical for driving CASP11-dependent protective responses against *Burkholderia thailandensis* (Aachoui et al., 2015). The amplified IFN $\gamma$ -mediated response in macrophages is specific to CASP11 inflammasome activation as IFN $\gamma$  priming has no effect on NLRP3 activity. We provide evidence that, although IFN $\gamma$  promotes the expression of CASP11, the priming effects of IFN $\gamma$  extend beyond CASP11 upregulation. Moreover, IFN $\gamma$  priming significantly enhances CASP11-dependent responses compared with IFN $\beta$  or LPS priming in BMDMs lacking CASP1 or all GBPs encoded on chromosome 3, which includes the homolog of human GBP1. Overall, we conclude that IFN $\gamma$  priming specifically promotes rapid CASP11-dependent pyroptosis in response to cytosolic LPS by a process that is independent of GBPs encoded on chromosome 3 or its ability to upregulate CASP11 expression. An unknown IFN $\gamma$ -inducible factor likely contributes to CASP11 activation and pyroptosis in response to cytosolic LPS.

## RESULTS

### IFN $\gamma$ Is a Potent Priming Agent for the Response to Cytosolic LPS in Macrophages

To study inflammasome-dependent pyroptosis, researchers have historically primed macrophages with a variety of TLR agonists, recombinant IFNs or cytokines (Latz et al., 2013). Priming is understood to transcriptionally upregulate the expression of critical inflammasome components. For example, the expression of NLRP3 and IL-1 $\beta$  are transcriptionally upregulated by TLR ligands or TNF, a key step for NLRP3 inflammasome activation (Bauernfeind et al., 2009, 2016). Priming for CASP11-dependent pyroptosis can be achieved with TLR agonists, such as LPS, or recombinant IFNs, which induce the expression of CASP11. Mechanistically, LPS upregulates CASP11 expression indirectly via TLR4-dependent TRIF signaling and the production of type I IFNs, highlighting the importance of IFN signaling in CASP11 expression (Rathinam et al., 2012; Broz et al., 2012). IFN $\gamma$ , the sole type II IFN, is a well-established activator of macrophages and also primes bone marrow-derived macrophages (BMDMs) for the CASP11-dependent response to cytosolic LPS (Schauvliege et al., 2002; Rathinam et al., 2012; Meunier et al., 2014). Despite our understanding that priming is important for both NLRP3 and CASP11-dependent inflammasome activation and pyroptosis, little is known about how these priming agents differ in their ability to promote these distinct processes.

To further characterize differences between priming conditions, we set out to determine the relative abilities of IFNs and TLR ligands to promote NLRP3- and CASP11-dependent inflammasome activation and pyroptosis. Based on previously published priming conditions, we treated primary BMDMs for 16 h with IFN $\gamma$  (100 U/mL), IFN $\beta$  (100 U/mL), or LPS (10 ng/mL) and monitored NLRP3- or CASP11-dependent inflammasome activation. As expected, LPS priming significantly increased NLRP3-induced BMDM cell death (measured by release of lactate dehydrogenase; LDH) 2 h after treatment with the classical NLRP3 activators, ATP or Nigericin (Figure 1A). IL-18 and IL-1 $\beta$  cytokine release, which are associated with inflammasome activation, were also significantly higher 2 h after NLRP3 activation in BMDMs primed with LPS (Figures 1B and 1C). These results are in line with previous publications demonstrating that LPS is a potent priming agent for NLRP3 inflammasome activation. However, neither IFN $\gamma$  nor IFN $\beta$  promoted NLRP3 inflammasome activation as determined by cell death or cytokine release 2 h after activation (Figures 1A–1C). The kinetics of cell death monitored by the incorporation of SYTOX Green further support the conclusion that LPS, but not IFN $\gamma$  or IFN $\beta$ , primes BMDMs for NLRP3

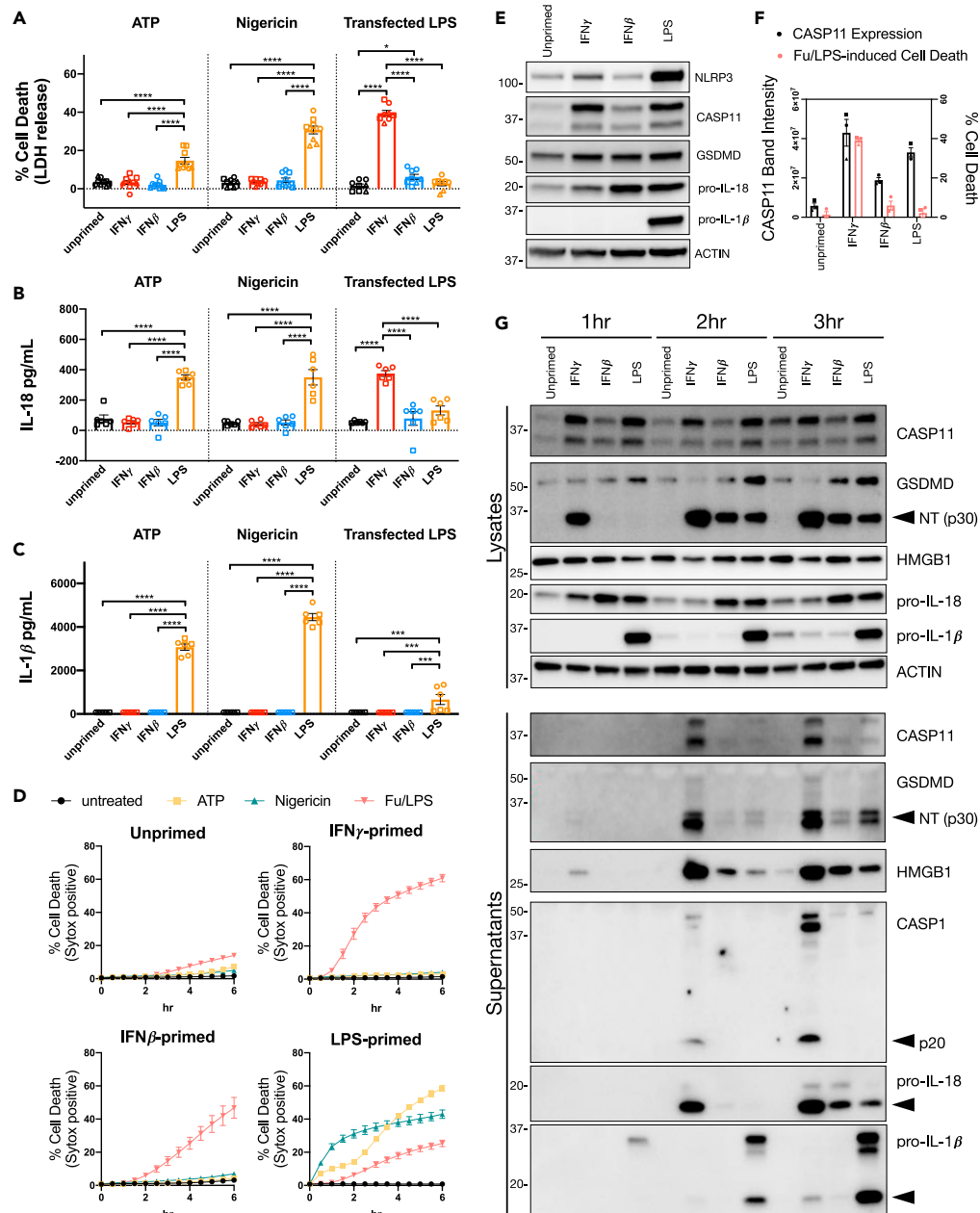


**Figure 1. IFN $\gamma$  is a Potent Priming Agent for the Response to Cytosolic LPS in Macrophages**

(A–D) WT BMDMs were primed for 16 h overnight with the following treatments: unprimed (N/A), IFN $\gamma$  (100 U/mL), IFN $\beta$  (100 U/mL), or LPS (10 ng/mL). NLRP3 and CASP11 inflammasome activation was triggered with ATP (5 mM), Nigericin (10  $\mu$ M), or by LPS (*E. coli* 0111:B4, 25  $\mu$ g/mL) transfection with FuGENE HD (Fu/LPS). At 2 h following inflammasome activation, supernatants were collected to measure release of (A) lactate dehydrogenase (LDH) for percent cell death calculations, (B) IL-18, and/or (C) IL-1 $\beta$ . (D) Cell death kinetics were monitored over time following inflammasome activation by measuring the incorporation of SYTOX Green.

(E) Cell lysates were collected from BMDMs treated for 16 h of priming as described above and separated by SDS-PAGE. Western blot analysis was performed to determine protein expression of critical inflammasome components: NLRP3, CASP11, GSDMD, pro-IL-18, pro-IL-1 $\beta$ , and the loading control ACTIN.

(F) Quantitation of CASP11 expression was compared with CASP11-induced cell death by LPS transfection (Fu/LPS). Bar graphs in black correspond to the left axis, which represents CASP11 expression as band intensity normalized to ACTIN. The mean percent cell death at 2 h following LPS transfection (from the three independent experiments shown in A) are plotted in pink and correspond to the right axis.

**Figure 1. Continued**

(G) WT BMDMs were primed and transfected with LPS (*E. coli* 0111:B4, 25  $\mu\text{g}/\text{mL}$ ) as described for (A–D), then supernatants and lysates were collected at 1, 2, 3 h post transfection to monitor for the cleavage and release of inflammasome-related proteins by SDS-PAGE and western blot. Molecular weight marker positions are shown to the left of each blot, and arrows indicate a cleavage product. Bar graphs show the mean value  $\pm$  SEM along with individual data points pooled from independent experiments depicted with different shapes (A–C and F). Line graphs show the mean  $\pm$  SD of three technical replicates (D). Data were pooled from three (A and F) or two (B and C) independent experiments or are representative of three (D and E) or two (G) independent experiments. Statistical analysis performed using a two-way ANOVA and Tukey's multiple comparisons test; \*\*\*\*  $< 0.0001$ ; \*\*\* = 0.0002–0.0001; \* = 0.0463. See also [Figure S1](#).

inflammasome activation ([Figure 1D](#)). Interestingly, we observed a different pattern of cell death and cytokine release using the same priming conditions for CASP11 inflammasome activation by transfected LPS.  $\text{IFN}\gamma$  priming significantly increased cell death and IL-18 release following LPS transfection compared with BMDMs primed with LPS or  $\text{IFN}\beta$  or left unprimed ([Figures 1A](#) and [1B](#)). However, IL-1 $\beta$  release following LPS transfection was only detected in BMDMs primed with LPS ([Figure 1C](#)). Monitoring cell death at later time points demonstrates that priming with  $\text{IFN}\beta$  or LPS also promotes cell death in response to transfected LPS, which is in line with previous reports ([Figure 1D](#)). However, BMDMs primed with  $\text{IFN}\gamma$  and subsequently transfected with LPS die at a faster rate and to a greater extent than BMDMs primed with  $\text{IFN}\beta$  or LPS ([Figures 1A](#) and [1D](#)). These data demonstrate that inflammasome complex activation is differentially regulated by the macrophage priming agents  $\text{IFN}\gamma$ ,  $\text{IFN}\beta$ , and LPS. For example, NLRP3 inflammasome activation could only be promoted with LPS, whereas all three priming agents promoted CASP11 inflammasome activation. Interestingly, these priming conditions promoted CASP11 inflammasome activation to different extents, with  $\text{IFN}\gamma$  priming inducing the most potent response.

Since priming is known to induce the expression of critical inflammasome components, we sought to determine how  $\text{IFN}\gamma$ ,  $\text{IFN}\beta$ , and LPS differentially regulate these proteins as a way to mechanistically explain inflammasome activation differences. To this end, primary BMDMs were treated for 16 h with  $\text{IFN}\gamma$ ,  $\text{IFN}\beta$ , or LPS as described above and cell lysates were separated by SDS-PAGE for western blot. As expected, LPS priming increased the expression of NLRP3 compared with priming with  $\text{IFN}\gamma$  or  $\text{IFN}\beta$  ([Figure 1E](#)). Therefore, the difference between  $\text{IFN}\gamma$ ,  $\text{IFN}\beta$ , and LPS priming on NLRP3 inflammasome activation can in part be attributed to the ability or inability of a priming agent to induce the expression of NLRP3. Furthermore, the expression of pro-IL-1 $\beta$  is highly induced by LPS priming, demonstrating that release of IL-1 $\beta$  is not a good marker of inflammasome activation when BMDMs are primed with  $\text{IFN}\gamma$  or  $\text{IFN}\beta$  ([Figures 1C](#) and [1E](#)). Although the expression of pro-IL-18 is increased by priming with  $\text{IFN}\beta$  or LPS, expression levels between priming conditions are more similar making the release of IL-18 a better marker of inflammasome activation when comparing conditions of priming ([Figures 1B](#) and [1E](#), [S1A](#), and [S1C](#)). As expected, the expression of CASP11 was induced by  $\text{IFN}\gamma$ ,  $\text{IFN}\beta$ , and LPS priming ([Figure 1E](#)). The two CASP11 proteins detected by western blot represent the full-length protein and an N-terminally truncated isoform generated by alternative translation similar to isoforms generated by the transcript encoding MAVS (data not shown) ([Brubaker et al., 2014](#); [Kang et al., 2000](#)). In contrast to the induction of CASP11 by priming, GSDMD expression remained constant as described previously ([Kayagaki et al., 2019](#)). By comparing CASP11 expression with cell death 2 h following LPS transfection (Fu/LPS), we found that the percentage of cell death correlated with the level of CASP11 expression for  $\text{IFN}\gamma$ -primed BMDMs ([Figure 1F](#)). However, the percentage of cell death at 2 h following LPS transfection was barely elevated for  $\text{IFN}\beta$ - or LPS-primed BMDMs despite higher levels of CASP11 expression ([Figure 1F](#)). These data suggest that other factors in addition to CASP11 regulate the response to cytosolic LPS. We also conducted a dose titration of priming agents to compare CASP11 expression and cell death at 3 h following LPS transfection ([Figures S1A–S1D](#)). LPS induced high levels of CASP11 expression; however, LPS-induced cell death by transfection was much lower compared with similar levels of CASP11 priming by  $\text{IFN}\gamma$  ([Figures S1A](#) and [S1B](#)). In contrast, priming with  $\text{IFN}\beta$  required much higher concentrations compared with  $\text{IFN}\gamma$  to induce similar levels of CASP11 expression and to induce equivalent levels of LPS-induced cell death ([Figures S1C](#) and [S1D](#)).

Further supporting the notion that  $\text{IFN}\gamma$  is the most potent promoter of CASP11 inflammasome activation, we found that increased cell death by  $\text{IFN}\gamma$  priming correlated with GSDMD cleavage. Cleaved NT-GSDMD accumulated more rapidly in cell lysates from  $\text{IFN}\gamma$ -primed BMDMs transfected with LPS compared with  $\text{IFN}\beta$  or LPS primed BMDMs ([Figure 1G](#)). In addition, the release of CASP11, NT-GSDMD, HMGB1, cleaved CASP1, and cleaved IL-18 was higher in supernatants from BMDMs primed

with IFN $\gamma$  compared with IFN $\beta$  or LPS (Figure 1G). Release of cleaved IL-1 $\beta$  into the supernatants was highest in LPS-primed BMDMs; however, this can be explained by the dramatic difference in pro-IL-1 $\beta$  expression between priming agents (Figures 1E and 1G). Collectively, these data demonstrate that IFN $\gamma$  is a potent priming agent for the response to cytosolic LPS in BMDMs.

### IFN $\gamma$ Priming Specifically Promotes CASP11 Inflammasome Activation

Previous publications have demonstrated that the murine BMDM inflammasome response to cytosolic LPS requires CASP11 activity and GSDMD. Once cleaved by CASP11, the NT-GSDMD fragment generates pores in the plasma membrane causing a K<sup>+</sup> efflux that triggers NLRP3-dependent CASP1 inflammasome activation (Ruhl and Broz, 2015). Thus, the response to cytosolic LPS is associated with downstream CASP1 activity, which contributes to cell death as well as the release of bioactive IL-18 and IL-1 $\beta$  (Kayagaki et al., 2011; Ruhl and Broz, 2015). Since IFN $\gamma$  priming did not promote NLRP3 inflammasome activation with classic NLRP3 agonists (Figures 1A–1D), we speculated that the effect of IFN $\gamma$  may specifically promote CASP11 inflammasome activation rather than promoting downstream NLRP3/CASP1 inflammasome activation. To test this hypothesis, we compared CASP11 inflammasome activation by transfected LPS in WT, *Casp1*<sup>−/−</sup>, and *Casp11*<sup>−/−</sup> BMDMs. In line with our previous results, IFN $\gamma$  priming significantly increased WT BMDM cell death (measured by release of LDH) and release of IL-18 3 h after LPS transfection compared with unprimed, IFN $\beta$ -primed, or LPS primed WT BMDMs (Figures 2A and 2B). The release of IL-1 $\beta$  was only detected in WT BMDMs primed with LPS (Figure 2C). However, as described earlier, IFN $\gamma$  and IFN $\beta$  do not induce the expression of pro-IL-1 $\beta$ , making release of IL-1 $\beta$  an unreliable marker of inflammasome activation when comparing these priming conditions (Figures 1E and 2E). As expected, cell death and IL-18 release following LPS transfection was completely dependent on CASP11 regardless of the priming condition used (Figures 2A and 2B). Furthermore, IL-18 and IL-1 $\beta$  release were completely dependent on CASP1, which is consistent with its role in cleaving these cytokines and promoting their secretion (Kayagaki et al., 2011; Ruhl and Broz, 2015). There was a significant decrease in the level of cell death following LPS transfection when comparing WT with *Casp1*<sup>−/−</sup> BMDMs primed with IFN $\gamma$  (Figure 2A). This result is consistent with a role for NLRP3-dependent sensing of K<sup>+</sup> efflux contributing to the cytosolic LPS response observed previously (Ruhl and Broz, 2015). However, there were significant differences in the cell death response to cytosolic LPS when CASP1-deficient BMDMs were primed with IFN $\gamma$ , IFN $\beta$ , or LPS (Figure 2A). Similar to WT BMDMs, IFN $\gamma$  priming in *Casp1*<sup>−/−</sup> BMDMs promoted a faster rate and greater magnitude of cell death compared with priming with IFN $\beta$  or LPS (Figures 2A and 2D). Importantly, the levels of CASP11 expression in CASP1-deficient BMDMs primed with IFN $\gamma$  and LPS were similar, suggesting that a factor other than CASP11 controls the differential response seen between IFN $\gamma$  and LPS priming (Figure 2E). Collectively, these data support the conclusion that IFN $\gamma$  priming specifically promotes CASP11 activation in response to transfected LPS independent of NLRP3 and CASP1.

We considered whether IFN $\gamma$  priming might specifically promote delivery of LPS to the cytosol during transfection. Using a FITC-labeled LPS conjugate, we found that IFN $\gamma$  priming did not increase the amount of FITC-LPS recovered from transfected BMDMs (Figure S2A). Therefore, IFN $\gamma$  does not simply promote ligand binding by increasing the efficiency of LPS transfection.

NT-GSDMD pore formation occurs downstream of GSDMD cleavage but upstream of NLRP3 inflammasome activation (Kayagaki et al., 2015). Comparing the kinetics of GSDMD cleavage between differentially primed BMDMs (Figure 1G) suggested to us that IFN $\gamma$  promotes a mechanism upstream of NT-GSDMD rather than pore formation itself. To directly test if IFN $\gamma$  treatment regulates NT-GSDMD pore formation, we generated a cell line in *Gsdmd*-CRISPR/Cas9 KO RAW cells that expresses the NT-GSDMD fragment under a Doxycycline-inducible promoter. These NT-GSDMD inducible cells were either primed with IFN $\gamma$  or left unprimed for 16 h, then treated with increasing concentrations of Doxycycline to induce the expression of NT-GSDMD and monitored for cell death (Figure S2B). IFN $\gamma$  had no effect on cell death following Doxycycline treatment, demonstrating that NT-GSDMD pore formation proceeds independently of IFN $\gamma$  priming. These data suggest that IFN $\gamma$  promotes CASP11-dependent pyroptosis upstream of NT-GSDMD pore formation.

### Priming Promotes Cell Death in Response to Cytosolic LPS Independently of CASP11 Expression

We observed that the kinetics and extent of pyroptosis in WT BMDMs in response to cytosolic LPS did not always correlate directly with the level of CASP11 expression following treatment with IFN $\gamma$ , IFN $\beta$ , or LPS (Figures 1A, 1B, 1D–1F, and S1A–S1D). These findings suggest that another factor or factors dependent on priming may promote the response to cytosolic LPS independently of CASP11 expression. To test this

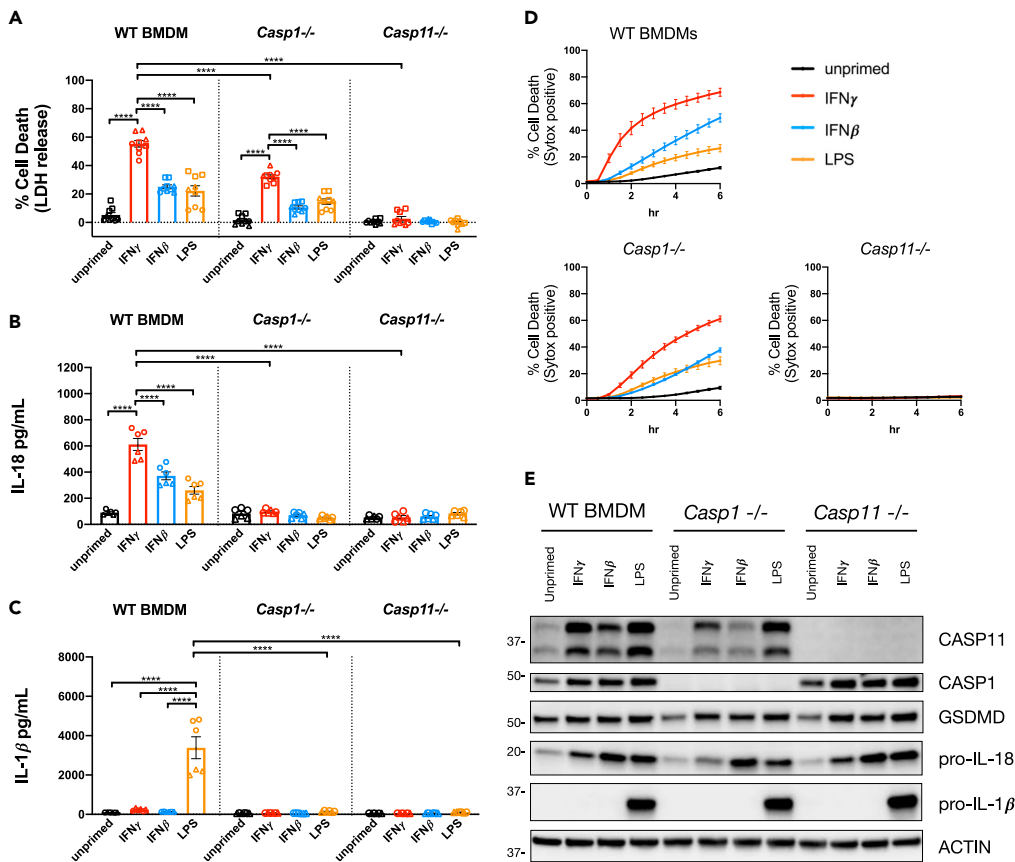


### Figure 2. IFN $\gamma$ Priming Specifically Promotes CASP11 Inflammasome Activation

(A–D) WT, *Casp1*<sup>-/-</sup>, and *Casp11*<sup>-/-</sup> BMDMs were primed for 16 h overnight with the following treatments: unprimed (N/A), IFN $\gamma$  (100 U/mL), IFN $\beta$  (100 U/mL), or LPS (10 ng/mL). CASP11 inflammasome activation was triggered by LPS (*E. coli* 0111:B4, 25 $\mu$ g/mL) transfection with FuGENE HD. At 3 h following inflammasome activation, supernatants were collected to measure release of (A) LDH for percent cell death calculations, (B) IL-18, and/or (C) IL-1 $\beta$ . (D) Cell death kinetics were monitored over time following inflammasome activation by measuring the incorporation of SYTOX Green. (E) Cell lysates were collected from WT, *Casp1*<sup>-/-</sup>, or *Casp11*<sup>-/-</sup> BMDMs treated for 16 h of priming as described above and separated by SDS-PAGE. Western blot analysis was performed to determine protein expression of critical inflammasome components: CASP11, CASP1, GSDMD, pro-IL-18, pro-IL-1 $\beta$ , and the loading control ACTIN. Molecular weight marker positions are shown to the left of each blot. Bar graphs show the mean value  $\pm$  SEM along with individual data points pooled from independent experiments depicted with different shapes (A–C). Line graphs show the mean value  $\pm$  SEM from pooled independent experiments with technical triplicates (D). Data were pooled from three (A and D) or two (B and C) independent experiments or are representative of three independent experiments (E). Statistical analysis performed using a two-way ANOVA and Tukey's multiple comparisons test; \*\*\*\* <0.0001. See also Figure S2.

hypothesis directly, we set out to generate a cell line that constitutively expresses CASP11 from a retroviral expression vector to uncouple the expression of CASP11 from priming. To this end, we chose to use RAW 264.7 cells, which are more amenable to genetic manipulations. Importantly, this immortalized cell line behaves similarly to WT BMDMs in our assays despite requiring a higher concentration of IFN $\beta$  to induce comparable levels of CASP11 expression (Figures S3A–S3E). IFN $\gamma$  priming of RAW 264.7 cells promoted faster kinetics and higher levels of cell death in response to cytosolic LPS delivered by transfection or with the Cholera Toxin B (CTB) subunit as compared with unprimed, IFN $\beta$ -primed, or LPS-primed cells (Figures S3B and S3C). CTB-mediated delivery of LPS to activate CASP11 has been described previously (Kayagaki et al., 2013; Hagar et al., 2013). In addition, similar to observations in WT BMDMs (Figure S2A), IFN $\gamma$  did not appear to increase the efficiency of LPS transfection into RAW 264.7 as measured with a FITC-labeled LPS conjugate capable of inducing CASP11-dependent inflammasome activation (Figures S3D and S3E). Thus, the immortalized RAW 264.7 cell line is a suitable background to uncouple the expression of CASP11 from priming and test if priming can still influence the response to cytosolic LPS.

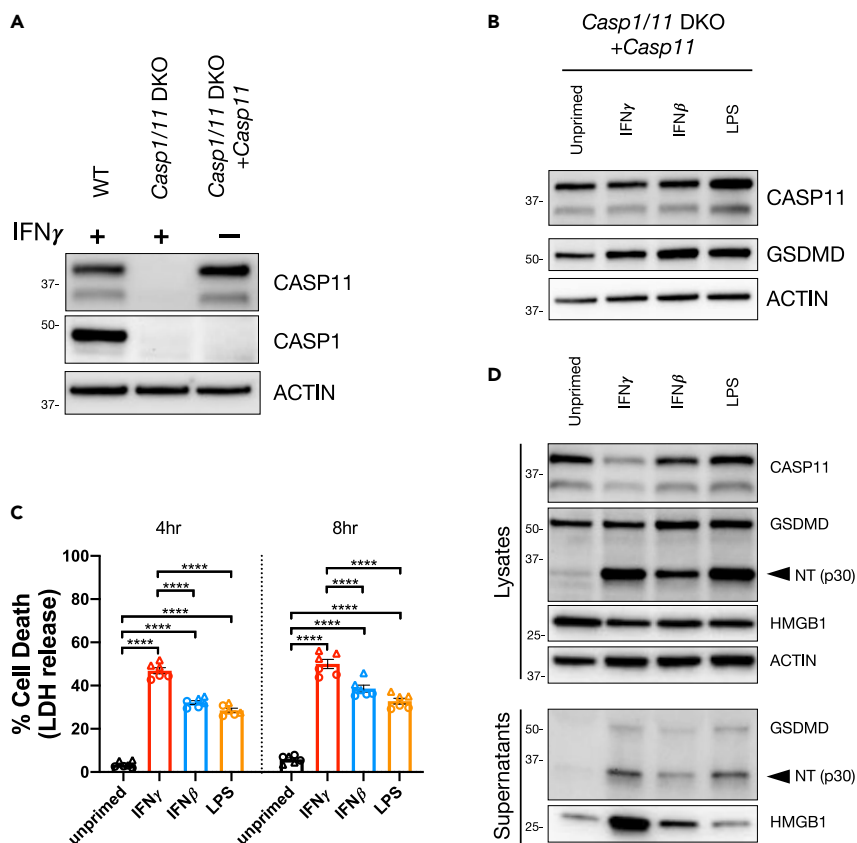


**Figure 3. Priming Promotes Cell Death in Response to Cytosolic LPS Independently of CASP11 Expression**

A constitutive CASP11-expressing cell line was generated by transducing a CASP11 expression vector into *Casp1,Casp11*-CRISPR/Cas9 DKO RAW cells (*Casp1/11* DKO).

(A) Cell lysates were collected from WT, *Casp1/11* DKO, and the constitutive cell line (*Casp1/11* DKO + *Casp11*) and analyzed by western blot to determine CASP1 and CASP11 expression. WT and *Casp1/11* DKO were treated with IFN $\gamma$  (100 U/mL) for 16 h.

(B) The constitutive CASP11-expressing cell line was primed for 16 h overnight with the following treatments; unprimed (N/A), IFN $\gamma$  (100 U/mL), IFN $\beta$  (1,000 U/mL), or LPS (10 ng/mL). Lysates were collected to determine the effects of priming on CASP11 expression by western blot.

(C and D) The constitutive CASP11-expressing cell line was primed as described above and CASP11 inflammasome activation was triggered by LPS (*E. coli* 0111:B4, 50  $\mu$ g/mL) transfection with FuGENE HD. (C) At 4 and 8 h following inflammasome activation, supernatants were collected to measure release of LDH for percent cell death calculations. (D) Alternatively, supernatants and lysates were collected 3 h post transfection to monitor for the cleavage and release of inflammasome-related proteins by SDS-PAGE and western blot. Molecular weight marker positions are shown to the left of each blot, and arrows indicate a cleavage product. Bar graphs show the mean value  $\pm$  SEM along with individual data points pooled from independent experiments depicted with different shapes (C). Data were pooled from two (C) independent experiments or are representative of three (A and B) or two (D) independent experiments.

Statistical analysis performed using a two-way ANOVA and Tukey's multiple comparisons test; \*\*\*\* <0.0001. See also Figure S3.

To generate the CASP11 constitutive cell line, we transduced *Casp1,Casp11*-CRISPR/Cas9 DKO RAW macrophages with a construct that constitutively drives CASP11 expression and selected for a clone with stable expression similar to that observed in WT RAW 264.7 cells primed with IFN $\gamma$  (Figure 3A). There were minimal changes to CASP11 and GSDMD expression when this cell line was primed with IFN $\gamma$ , IFN $\beta$ , or LPS (Figure 3B). Despite this, each of the priming agents promoted cell death following LPS transfection as observed by the release of LDH and GSDMD cleavage (Figures 3C and 3D). In support of our hypothesis that IFN $\gamma$  is the most potent promoter of CASP11 inflammasome activation, IFN $\gamma$  priming resulted in significantly higher levels of cell death in this cell line compared with IFN $\beta$  or LPS priming (Figure 3C). In addition, higher amounts of HMGB1 were released from IFN $\gamma$ -primed cells compared with IFN $\beta$  or LPS priming



(Figure 3D). Similar results were obtained when cytosolic LPS was delivered with CTB (Figures S3F and S3G). Specifically, IFN $\gamma$  priming promoted higher levels of cell death, GSDMD cleavage, and release of HMGB1 (Figures S3F and S3G). Because this constitutive CASP11-expressing cell line is CASP1 deficient, these data further support our conclusion that IFN $\gamma$  specifically promotes CASP11-dependent cell death independently of CASP1. By genetically uncoupling the ability of priming agents to induce CASP11 expression, these data demonstrate that IFN $\gamma$  promotes rapid pyroptosis in response to cytosolic LPS through an unknown mechanism that is separate from its ability to induce CASP11 expression.

### IFN $\gamma$ Receptor Signaling Enhances but Is Not Required for CASP11 Inflammasome Activation

Our data demonstrate that IFN $\gamma$  priming enhances CASP11 inflammasome activation in response to cytosolic LPS. To identify genes required for this enhanced response to cytosolic LPS, we utilized the GeCKOv2 pooled gRNA library to generate and screen a genome-wide CRISPR knockout library in the constitutive CASP11-expressing cell line described in Figure 3 (Sanjana et al., 2014). We conducted survival screens by activating the cell death response to cytosolic LPS with or without IFN $\gamma$  priming. Enrichment of gRNAs in the surviving cell populations was determined using the MAGeCK algorithm (Li et al., 2014). Cells containing gRNAs that target the IFN $\gamma$  receptor-encoding genes, *Ifngr1* and *Ifngr2*, were highly enriched with IFN $\gamma$  priming compared with the unprimed condition (Figure S4). More specifically, there was no enrichment of *Ifngr1* and *Ifngr2* gRNA-containing cells following CASP11 inflammasome activation without IFN $\gamma$  priming. These data suggest that IFN $\gamma$  receptor signaling is not required for CASP11 inflammasome activation but is required for the IFN $\gamma$  enhanced response against cytosolic LPS.

IFN $\gamma$  induces a pleiotropic set of transcriptional, translational, and metabolic changes in macrophages by binding and signaling through a heterodimer receptor complex composed of IFN $\gamma$ R1 and IFN $\gamma$ R2 (Schroder et al., 2004; Su et al., 2015). Based on our CRISPR screen results, we suspected that signaling through this receptor complex enhances but is not absolutely critical for the response to cytosolic LPS. To formally test this hypothesis, we compared the response to cytosolic LPS between WT and *Ifngr1*<sup>-/-</sup> BMDMs (Huang et al., 1993). Compared with WT BMDMs, there was a significant reduction in cell death following LPS transfection in *Ifngr1*<sup>-/-</sup> BMDMs primed with IFN $\gamma$  (Figure 4A). This result is not surprising, given that CASP11 expression was not induced in *Ifngr1*<sup>-/-</sup> BMDMs primed with IFN $\gamma$  as compared with WT BMDMs (Figure 4B). If we primed *Ifngr1*<sup>-/-</sup> BMDMs with IFN $\beta$  or LPS, however, CASP11 expression was induced and there was a significant increase in the cell death response to cytosolic LPS compared with unprimed *Ifngr1*<sup>-/-</sup> BMDMs (Figures 4A and 4B). Furthermore, there was no significant difference in the cell death response to cytosolic LPS between WT and *Ifngr1*<sup>-/-</sup> BMDMs when cells were primed with IFN $\beta$  or LPS (Figure 4A). These data provide evidence that IFN $\gamma$  receptor signaling is not critical for the response to cytosolic LPS but rather enhances it.

Monitoring the kinetics of cell death following LPS transfection also supports the conclusion that IFN $\gamma$  receptor signaling is not critical for the response to cytosolic LPS. As we observed previously, WT BMDMs primed with IFN $\gamma$  exhibited the most rapid cell death response to transfected LPS compared with IFN $\beta$ -, LPS-, or unprimed BMDMs (Figure 4C). The kinetics of cell death for IFN $\gamma$  receptor-deficient BMDMs were similar to WT BMDMs when primed with IFN $\beta$  or LPS, whereas *Ifngr1*<sup>-/-</sup> BMDMs primed with IFN $\gamma$  died at a rate similar to unprimed BMDMs. These data demonstrate that IFN $\gamma$  receptor signaling is only required to promote rapid cell death in response to cytosolic LPS when BMDMs are primed with IFN $\gamma$  (Figure 4C). Finally, unprimed WT and *Ifngr1*<sup>-/-</sup> BMDMs undergo similar cell death kinetics in response to transfected LPS compared with LPS treatment alone (Figure 4D). Thus, IFN $\gamma$  receptor signaling is not required for basal responses to cytosolic LPS in the absence of priming. Collectively, our data demonstrate that IFN $\gamma$  receptor signaling is not critical for CASP11 activation but suggest that IFN $\gamma$  priming induces the expression or activation of an unknown factor that enhances the response to cytosolic LPS.

### IFN $\gamma$ Enhancement of CASP11-Dependent Pyroptosis Requires GSDMD and Is Independent of GSDME

Pyroptosis as an outcome of inflammasome activation has primarily been attributed to cleavage of GSDMD by CASP11 or CASP1 (Shi et al., 2015; Kayagaki et al., 2015). Following cleavage, the N-terminal fragment of GSDMD forms pores in the plasma membrane resulting in pyroptotic cell death, and thus, BMDMs deficient for GSDMD are refractory to CASP11- or CASP1-induced pyroptosis (Shi et al., 2015; Kayagaki et al., 2015; Ding et al., 2016; Liu et al., 2016; Aglietti et al., 2016). Recent publications have now revealed that GSDME, a homolog of GSDMD, is cleaved by alternative cell death pathways and the GSDME

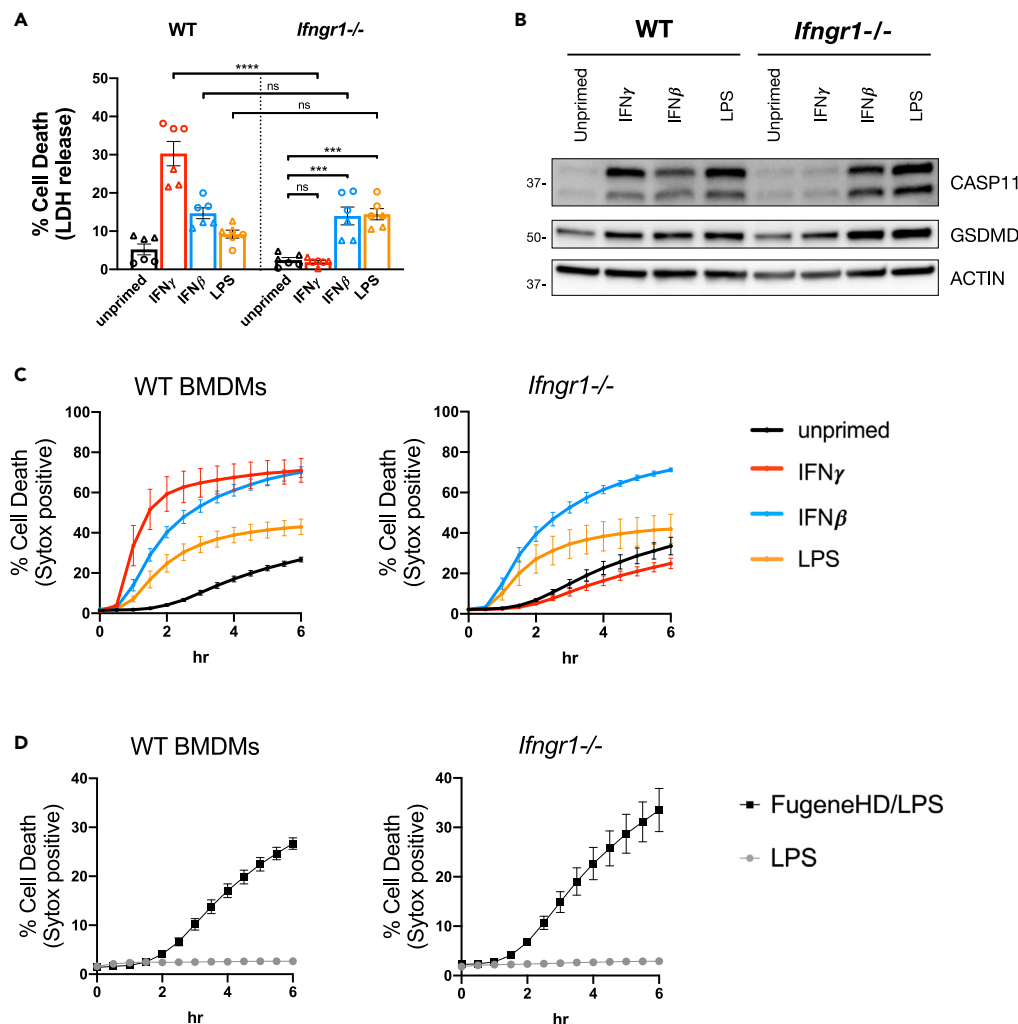


**Figure 4. IFN $\gamma$  Receptor Signaling Enhances but is not Required for CASP11 Inflammasome Activation**

(A, C, and D) WT and *Ifngr1*<sup>-/-</sup> BMDMs were primed for 16 h overnight with the following treatments: unprimed (N/A), IFN $\gamma$  (100 U/mL), IFN $\beta$  (100 U/mL), or LPS (10 ng/mL). CASP11 inflammasome activation was triggered by LPS (*E. coli* 0111:B4, 25  $\mu$ g/mL) transfection with FuGENE HD.

(A) At 2 h following inflammasome activation, supernatants were collected to measure release of LDH for percent cell death calculations.

(B) Cell lysates were collected from BMDMs treated for 16 h of priming as described above and separated by SDS-PAGE. Western blot analysis was performed to determine protein expression of CASP11, GSDMD, and the loading control ACTIN. Molecular weight marker positions are shown to the left of each blot.

(C and D) Cell death kinetics were monitored over time following inflammasome activation by measuring the incorporation of SYTOX Green. (C) Comparisons between different priming conditions are shown for BMDMs transfected with LPS. (D) Additionally, a comparison between unprimed WT and *Ifngr1*<sup>-/-</sup> BMDMs treated with or without transfection reagent are shown. Bar graphs show the mean value  $\pm$  SEM along with individual data points pooled from independent experiments depicted with different shapes (A). Line graphs show the mean  $\pm$  SD of three technical replicates (C and D). Data were pooled from two (A) independent experiments or are representative of two (B–D) independent experiments.

Statistical analysis performed using a two-way ANOVA and Tukey's multiple comparisons test; \*\*\*\* <0.0001; \*\*\* <0.002. See also Figure S4.

N-terminal fragment similarly causes a necrotic form of rapid cell death (Rogers et al., 2017; Wang et al., 2017; Sarhan et al., 2018; Aizawa et al., 2020). Based on these previous findings, we set out to determine whether the enhanced response to cytosolic LPS induced by IFN $\gamma$  priming strictly requires GSDMD or whether it may also depend on GSDME.

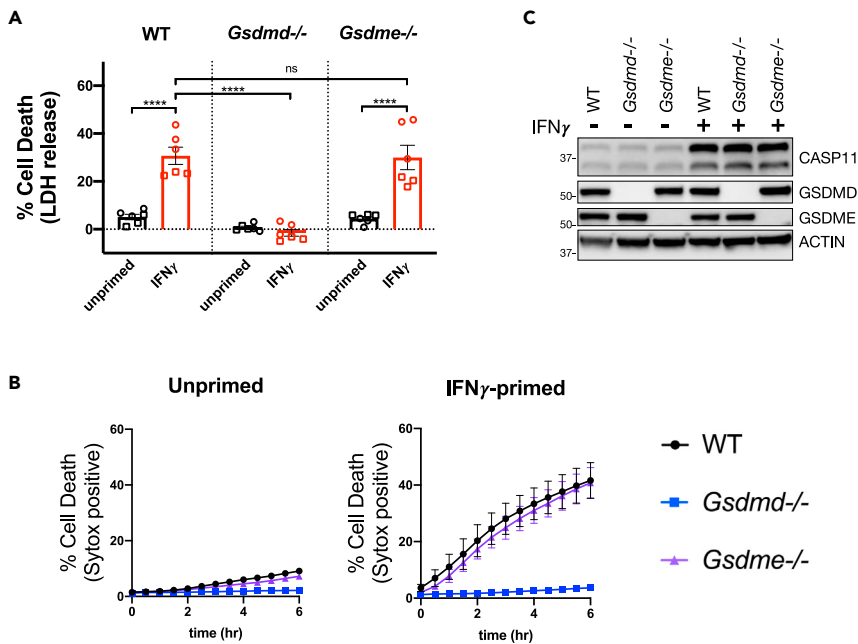


**Figure 5. IFN $\gamma$  Enhancement of CASP11-Dependent Cell Death Requires GSDMD and Is Independent of GSDME**

(A and B) WT, *Gsdmd*<sup>-/-</sup>, and *Gsdme*<sup>-/-</sup> BMDMs were primed for 16 h overnight with or without IFN $\gamma$  (100 U/mL). CASP11 inflammasome activation was triggered by LPS (*E. coli* 0111:B4, 25  $\mu$ g/mL) transfection with FuGENE HD. (A) At 4 h following inflammasome activation, supernatants were collected to measure release of LDH for percent cell death calculations. (B) Cell death kinetics were monitored over time following inflammasome activation by measuring the incorporation of SYTOX Green. (C) Cell lysates were collected from WT, *Gsdmd*<sup>-/-</sup>, or *Gsdme*<sup>-/-</sup> BMDMs treated for 16 h of priming as described above and separated by SDS-PAGE. Western blot analysis was performed to determine protein expression of CASP11, GSDMD, GSDME, and the loading control ACTIN. Molecular weight marker positions are shown to the left of each blot. Bar graphs show the mean value  $\pm$  SEM along with individual data points pooled from independent experiments depicted with different shapes (A). Line graphs show the mean  $\pm$  SEM from pooled independent experiments (B). Data were pooled from two (A and B) independent experiments or are representative of two independent experiments (C). Statistical analysis performed using a two-way ANOVA and Tukey's multiple comparisons test; \*\*\*\*  $<0.0001$ . See also Figure S5.

We began by comparing the cell death response to cytosolic LPS in WT, *Gsdmd*<sup>-/-</sup>, and *Gsdme*<sup>-/-</sup> BMDMs primed with or without IFN $\gamma$ . As expected, there were significantly lower levels of cell death at 4 h following LPS transfection in IFN $\gamma$ -primed BMDMs derived from *Gsdmd*<sup>-/-</sup> mice (Figure 5A). Monitoring the kinetics of cell death by SYTOX Green incorporation over time also demonstrated the absolute requirement of GSDMD for the response to IFN $\gamma$  priming and cytosolic LPS (Figure 5B). Although GSDMD was absolutely required, we observed no difference in cell death between WT and *Gsdme*<sup>-/-</sup> BMDMs primed with IFN $\gamma$  and transfected with LPS (Figures 5A and 5B). Importantly, CASP11 expression was similarly induced across all genotypes, eliminating the possibility that GSDMD and GSDME might control CASP11 expression in response to IFN $\gamma$  (Figure 5C). These data provide evidence that the enhanced CASP11-dependent response to cytosolic LPS induced by IFN $\gamma$  strictly requires GSDMD and is independent of GSDME.

As mentioned above, GSDME can be cleaved by alternative cell death pathways. For example, TAK1 inhibition in conjunction with TLR4 activation triggers an alternative CASP8/CASP3 cell death pathway in BMDMs that results in both GSDMD and GSDME cleavage (Sarhan et al., 2018; Orning et al., 2018). NLRP3 inflammasome activation in the absence of CASP1 activity provides another example in which macrophages switch to an alternative cell death pathway that triggers CASP8/CASP3 cleavage and relies on GSDMD as well as GSDME cleavage for cell death (Sagulenko et al., 2013; Schneider et al., 2017; Aizawa et al., 2020). Based on our results from experiments using *Gsdme*<sup>-/-</sup> BMDMs (Figures 5A–5C), we did not expect IFN $\gamma$  priming to promote cell death through the CASP8/CASP3/GSDME alternative cell death pathway. In support of this hypothesis, we found no evidence of CASP8, CASP3, or GSDME cleavage under

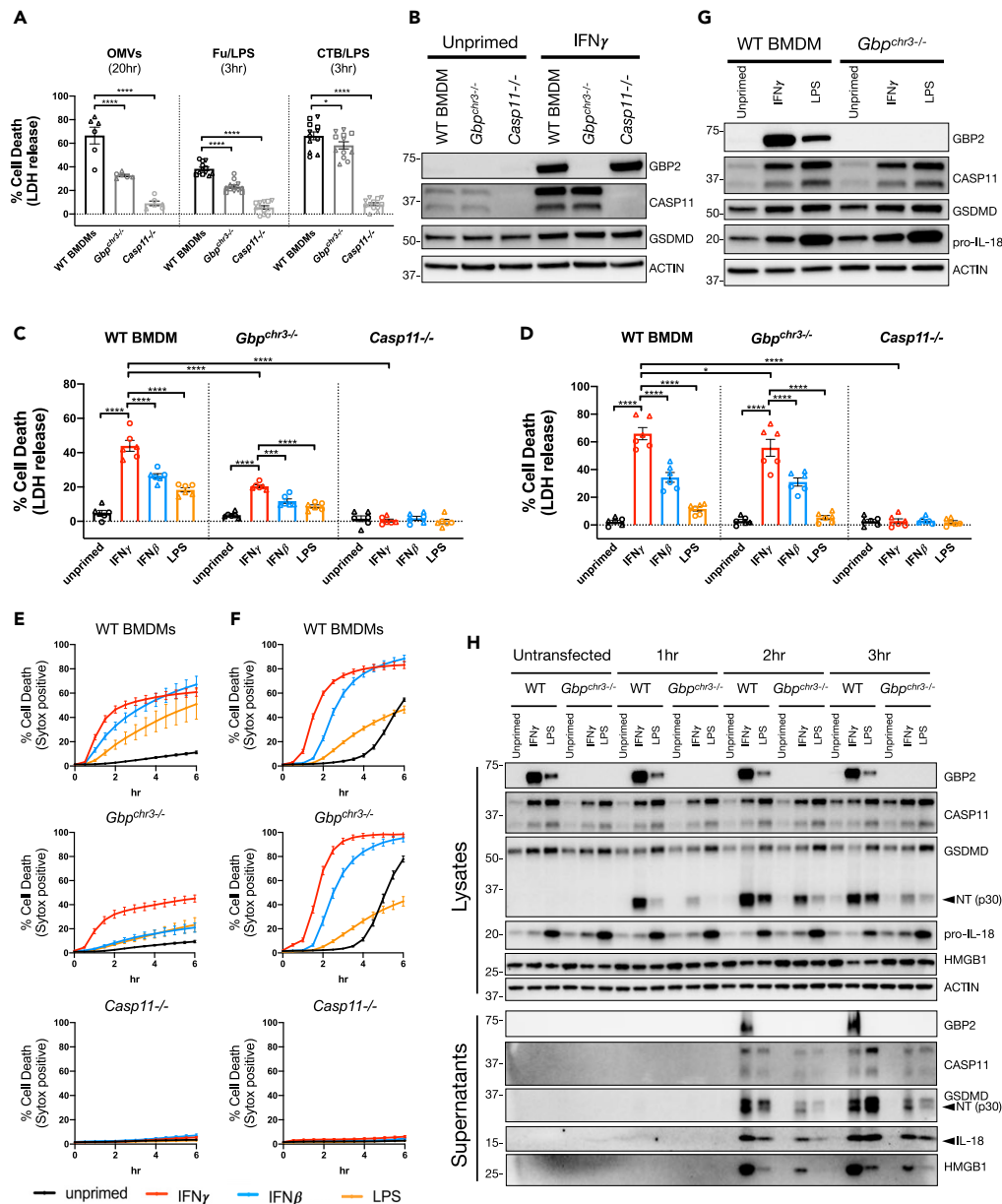


**Figure 6. GBPs Encoded on Chromosome 3 Do Not Fully Account for Enhanced CASP11-Dependent Cell Death Triggered by IFN $\gamma$  Priming**

(A and B) WT, *Gbpchr3*<sup>-/-</sup>, and *Casp11*<sup>-/-</sup> BMDMs were primed for 16 h overnight with or without IFN $\gamma$  (100U/mL). CASP11 inflammasome activation was triggered by treating cells with OMVs (*E. coli* DH5 $\alpha$ ), LPS (*E. coli* 0111:B4, 25  $\mu$ g/mL) transfection with FuGENE HD, or LPS (*E. coli* 0111:B4, 25  $\mu$ g/mL) mixed with CTB (Cholera Toxin B Subunit, 20  $\mu$ g/mL). (A) At the indicated time points following inflammasome activation, supernatants were collected to measure release of LDH for percent cell death calculations. (B) Cell lysates were collected from WT, *Gbpchr3*<sup>-/-</sup>, and *Casp11*<sup>-/-</sup> BMDMs treated with or without IFN $\gamma$  as described above and separated by SDS-PAGE. Western blot analysis was performed to determine protein expression of GBP2, CASP11, GSDMD, and the loading control ACTIN.

(C–F) WT, *Gbpchr3*<sup>-/-</sup>, and *Casp11*<sup>-/-</sup> BMDMs were primed for 16 h overnight with the following treatments: unprimed (N/A), IFN $\gamma$  (100 U/mL), IFN $\beta$  (100 U/mL), or LPS (10 ng/mL). CASP11 inflammasome activation was triggered by LPS transfection (C and E) or with CTB and LPS (D and F) as described above. Cell death was determined following inflammasome activation by collecting supernatants at 3 h to monitor LDH release (C and D), or cell death kinetics were monitored over time by measuring the incorporation of SYTOX Green (E and F).

**Figure 6. Continued**

(G) Cell lysates were collected from WT and *Gbpchr3*<sup>-/-</sup> BMDMs treated for 16 h of priming as described above and separated by SDS-PAGE. Western blot analysis was performed to determine protein expression of GBP2, CASP11, GSDMD, pro-IL-18, and the loading control ACTIN.

(H) WT and *Gbpchr3*<sup>-/-</sup> BMDMs were primed and transfected with LPS as described above. Supernatants and lysates were collected from untransfected, 1, 2, or 3 h post-transfection to monitor for the cleavage and release of inflammasome-related proteins by SDS-PAGE and western blot. Molecular weight marker positions are shown to the left of each blot, and arrows indicate a cleavage product. Bar graphs show the mean value  $\pm$  SEM along with individual data points pooled from independent experiments depicted with different shapes (A, C, and D). Line graphs show the mean value  $\pm$  SEM from pooled independent experiments with technical replicates (E and F). Data were pooled from four (A - Fu/LPS and CTB/LPS) or two (A - OMV, C, D, E, F) independent experiments or are representative of two (B and G) or one (H) independent experiment.

Statistical analysis performed using a two-way ANOVA and Tukey's multiple comparisons test; \*\*\*\* <0.0001; \*\*\* for (C) = 0.0005; \* for (A) = 0.0453; \* for (D) = 0.0294. See also [Figure S6](#).

IFN $\gamma$  priming conditions in our constitutively expressing CASP11 RAW 264.7 cell line or in WT BMDMs ([Figures S5A and S5B](#)). TAK1 inhibition by 5z7 or CASP1-deficient BMDMs were used as positive controls in these experiments to observe CASP8, CASP3, GSDME cleavage. In conditions where CASP8 and CASP3 were cleaved, we also detected the smaller p20 fragment of GSDMD, a product of CASP3 activity ([Sarhan et al., 2018](#); [Orning et al., 2018](#); [Chen et al., 2019](#)). Since IFN $\gamma$  priming does not directly promote NLRP3 inflammasome activation ([Figure 1](#)), cleavage of CASP8, CASP3, and GSDME in *Casp1*<sup>-/-</sup> BMDMs primed with IFN $\gamma$  and transfected with LPS is likely the result of downstream K<sup>+</sup> efflux-mediated NLRP3 activation, which switches to an alternative necrotic cell death pathway in the absence of CASP1 ([Ruhl and Broz, 2015](#); [Schneider et al., 2017](#); [Aizawa et al., 2020](#)).

Collectively, these data suggest that the enhanced CASP11-dependent response to cytosolic LPS that is triggered by IFN $\gamma$  priming strictly requires GSDMD for pyroptosis. This enhanced cell death response to IFN $\gamma$  priming and LPS transfection did not rely on GSDME and we found no evidence of GSDME cleavage that would suggest it plays a role in the process. Furthermore, the enhanced response to cytosolic LPS triggered by IFN $\gamma$  priming cannot be attributed to cleavage of CASP8 or CASP3, which constitute an alternative cell death pathway under certain conditions. Although it is possible that IFN $\gamma$  priming enhances the response to cytosolic LPS through a cell death pathway that has yet to be determined, our findings are consistent with the idea that IFN $\gamma$  specifically primes and enhances the CASP11-GSDMD-pyroptosis pathway.

**GBPs Encoded on Chromosome 3 Do Not Fully Account for Enhanced CASP11-Dependent Cell Death Triggered by IFN $\gamma$  Priming**

The guanylate-binding proteins (GBPs) have gained attention for their role during inflammasome activation in response to bacterial infection or in response to OMVs shed by Gram-negative bacteria ([Pilla et al., 2014](#); [Meunier et al., 2014](#); [Finethy et al., 2015, 2017](#); [Man et al., 2016](#); [Santos et al., 2018](#); [Cerqueira et al., 2018](#); [Tang et al., 2018](#); [Fisch et al., 2019](#); [Gu et al., 2019](#)). These proteins are highly upregulated in response to IFN $\gamma$  and are recruited to pathogen containing vacuoles and/or directly to bacteria during infection ([Tretina et al., 2019](#)). A subset of GBPs are required for CASP11 inflammasome activation in murine-derived BMDMs and are thought to play a role in facilitating CASP11-LPS interaction ([Santos et al., 2018](#); [Cerqueira et al., 2018](#)). Recent evidence in human cells demonstrates that GBP1 binds to LPS and assembles a signaling platform with several other GBPs for CASP4 activation ([Wandel et al., 2020](#); [Santos et al., 2020](#)). Based on these findings, we speculated that inducible GBPs could account for the increased level of CASP11-dependent pyroptosis we observe with IFN $\gamma$  priming ([Figures 1, 2, and 3](#)).

There are eleven highly conserved GBPs encoded in mice. Six of these are tandemly encoded on chromosome 3 and were collectively deleted to generate *Gbp*<sup>chr3-/-</sup> mice ([Yamamoto et al., 2012](#)). These mice have been used previously to demonstrate the importance of GBPs for inflammasome activation during bacterial infection ([Pilla et al., 2014](#); [Meunier et al., 2014, 2015](#); [Finethy et al., 2015](#); [Man et al., 2016](#)). Importantly, the closest homolog of human GBP1 is encoded within the chromosome 3 locus. Given the importance of human GBP1 in activating CASP4 ([Wandel et al., 2020](#); [Santos et al., 2020](#)), this may help to explain defects in CASP11 inflammasome activation during bacterial infection using *Gbp*<sup>chr3-/-</sup> BMDMs ([Pilla et al., 2014](#); [Meunier et al., 2014](#); [Finethy et al., 2015](#)). In line with previous reports, IFN $\gamma$  primed *Gbp*<sup>chr3-/-</sup> BMDMs displayed a partial defect in the cell death response to cytosolic LPS as triggered by treatment with

*E. coli*-derived OMVs, LPS transfection, or LPS complexed with CTB (Figure 6A and S6A) (Pilla et al., 2014; Finethy et al., 2017; Santos et al., 2018; Cerqueira et al., 2018; Tang et al., 2018; Gu et al., 2019). BMDMs derived from *Gbp<sup>chr3-/-</sup>* mice failed to upregulate Gbp2 when treated with IFN $\gamma$  but importantly express equivalent levels of CASP11 as compared with WT controls (Figure 6B). These data demonstrate that the interferon inducible GBPs encoded on chromosome 3 are partially required for CASP11 inflammasome activation when BMDMs are primed with IFN $\gamma$ . However, it remained to be determined whether the enhanced IFN $\gamma$  response to cytosolic LPS can be fully attributed to the function of these GBPs encoded on chromosome 3.

An important aspect of our current study lies in the comparison between different priming agents demonstrating that IFN $\gamma$  priming elicits the most rapid and amplified macrophage response to cytosolic LPS. For example, in testing *Casp1-/-* BMDMs we observed a partial defect in the cell death response following IFN $\gamma$  priming and LPS transfection (Figures 2A and 2D). However, we also compared the cell death response in *Casp1-/-* BMDMs using different priming agents and found significant differences between IFN $\gamma$  priming compared with IFN $\beta$  or LPS. Together these data demonstrate that CASP1 is involved in the response to cytosolic LPS (likely downstream of K<sup>+</sup> efflux as discussed above) but that CASP1 is not required for the differences observed between priming agents. Based on these results, we reasoned it would also be important to compare the response to cytosolic LPS using different priming agents in *Gbp<sup>chr3-/-</sup>* BMDMs to determine if the GBPs encoded on chromosome 3 are required for the enhanced cell death response observed with IFN $\gamma$  priming.

When comparing the effect of different priming agents, we found significant differences in the cell death response to cytosolic LPS in *Gbp<sup>chr3-/-</sup>* BMDMs. In line with our previous results, IFN $\gamma$  priming significantly increased CASP11-dependent cell death in WT BMDMs transfected with LPS or treated with CTB/LPS (Figures 6C and 6D). Similarly, IFN $\gamma$  priming promoted significantly higher levels of CASP11-dependent cell death in *Gbp<sup>chr3-/-</sup>* BMDMs compared with priming with IFN $\beta$  or LPS (Figures 6C and 6D). IFN $\gamma$  priming also promotes a more rapid CASP11-dependent response in *Gbp<sup>chr3-/-</sup>* BMDMs compared with other priming agents (Figures 6E and 6F). These data suggest that GBPs encoded on chromosome 3 are not required for the differential outcome observed between priming conditions. In line with results from WT and *Casp1-/-* BMDMs, the greatest difference in priming responses for CASP11 inflammasome activation in *Gbp<sup>chr3-/-</sup>* BMDMs lies between IFN $\gamma$  and LPS priming. Importantly, LPS priming induces equivalent levels of CASP11 expression, if not more, than IFN $\gamma$  priming in *Gbp<sup>chr3-/-</sup>* BMDMs (Figure 6G). Thus, the defect in CASP11-dependent responses using LPS priming conditions cannot be attributed to defects in CASP11 expression.

To confirm that IFN $\gamma$  priming promotes a more rapid and robust CASP11-dependent response independently of GBPs encoded on chromosome 3, we compared GSDMD cleavage over time and the release of cytokines from WT and *Gbp<sup>chr3-/-</sup>* BMDMs under different priming conditions. For the GSDMD cleavage experiment, we chose to focus on the difference between IFN $\gamma$  and LPS priming based on the greater phenotypic range between these conditions. Following LPS transfection, the N-terminal cleaved fragment of GSDMD accumulated more rapidly in WT BMDM lysates primed with IFN $\gamma$  compared with LPS priming, which confirms our previous results (Figures 6H and 1G). In support of our hypothesis, cleaved NT-GSDMD also accumulated more rapidly in the lysates of *Gbp<sup>chr3-/-</sup>* BMDMs primed with IFN $\gamma$  compared with LPS priming. Furthermore, the release of cleaved NT-GSDMD and HMGB1 into the supernatant was higher in *Gbp<sup>chr3-/-</sup>* BMDMs primed with IFN $\gamma$  compared with LPS priming (Figure 6H). An increased release of cleaved IL-18 from IFN $\gamma$ -primed *Gbp<sup>chr3-/-</sup>* BMDMs was more subtle but could be confirmed by an ELISA on supernatants collected at 3 h following CASP11 activation (Figures 6H and S6B).

Our data provide support to a growing body of research that demonstrate an important role for GBPs encoded on chromosome 3 in the response to cytosolic LPS by CASP11. However, we show that the enhanced CASP11-dependent response triggered by IFN $\gamma$  priming cannot solely be attributed to the function of GBPs encoded on chromosome 3. Interestingly, GBP1 is encoded within the chromosome 3 locus, which is of interest because its human homolog was recently shown to play an important role in assembling a GBP signaling platform with CASP4 and LPS (Wandel et al., 2020; Santos et al., 2020). Because *Gbp<sup>chr3</sup>* deficiency does not account for differences in CASP11-dependent responses between IFN $\gamma$ - and LPS-priming, our data suggest that an unknown factor(s) controls the differential response seen between these priming conditions.

## DISCUSSION

By comparing CASP11-dependent responses under different priming conditions, our study reveals specificity between these external cues that dictate inflammasome activation outcome. A key finding from our research is the demonstration that IFN $\gamma$  priming promotes the most rapid and robust CASP11-dependent response compared with IFN $\beta$  or LPS priming. Our results suggest that IFN $\gamma$  induces the activity of an unidentified CASP11 regulator that enhances pyroptosis in response to cytosolic LPS. This finding justifies a renewed search for unknown regulators of cytosolic LPS sensing, as the known regulators of this process cannot fully explain the priming effects of IFN $\gamma$ . Several lines of evidence support this conclusion. First, with the exception of complete CASP11 deficiency, we did not observe a direct correlation between the extent of CASP11 expression and the responsiveness of cells to different priming agents. Indeed, IFN $\gamma$  retained the ability to prime and increase pyroptosis levels in a cell line constitutively expressing CASP11. Furthermore, we provide evidence that GBPs encoded on chromosome 3 do not fully account for the enhanced effects of IFN $\gamma$  priming compared with IFN $\beta$  or LPS priming. We note, however, that we verify a role for GBPs encoded on chromosome 3 in CASP11 inflammasome activation as demonstrated by a partial defect in *Gbp<sup>chr3-/-</sup>* BMDMs response to cytosolic LPS (Pilla et al., 2014; Finethy et al., 2017; Santos et al., 2018; Cerqueira et al., 2018; Tang et al., 2018; Gu et al., 2019). Our results do not exclude the possibility that other interferon inducible GBPs (outside the chromosome 3 locus) are responsible for the enhancement of CASP11 responses driven by IFN $\gamma$  priming. There is no evidence to date, however, indicating a role in CASP11 function for these GBPs encoded outside chromosome 3. In conclusion, our data demonstrate that the observed IFN $\gamma$ -dependent increased response to transfected LPS must be controlled by a mechanism independent of its ability to control the expression of CASP11 or GBPs encoded on chromosome 3. Based on these findings we propose that IFN $\gamma$  priming induces the activity of an unknown CASP11 regulator(s).

Often with little regard to the priming step, the field of inflammasome research has primarily focused on the activation step and downstream effector functions, such as pyroptosis and cytokine release. Our data support previous research that demonstrates that priming agents differentially dictate inflammasome outcome (Figure 1) (Bauernfeind et al., 2009, 2016). To understand the biological relevance of these variable outcomes, future studies will likely require the use of *in vivo* models of infection. For example, Aachoui and colleagues provide compelling evidence that IFN $\gamma$  produced by NK and T cells *in vivo* is critically important to prime CASP11 and protect against infection using the model pathogen *Burkholderia thailandensis* (Aachoui et al., 2013, 2015; Kovacs et al., 2020). However, *in vivo* CASP11 responses can also be deleterious, causing higher rates of mortality in models of septic shock (Kayagaki et al., 2013; Hagar et al., 2013). Based on these diametrically opposed outcomes, the activation of CASP11 *in vivo* must be tightly regulated to provide protection when needed while simultaneously limiting collateral damage. Therefore, we speculate that the CASP11 response may have evolved a sensitivity to IFN $\gamma$  priming as a mechanism for gauging the level of infectious threat *in vivo*.

Transcription of *Casp11* is undoubtedly an important factor in tightly regulating the effects of CASP11, and yet our understanding of the promoter elements and transcription factors controlling expression is somewhat limited. Previous work demonstrates that CASP11 induced by LPS priming requires the nuclear factor  $\kappa$ B (NF- $\kappa$ B), the C/EBP homologous protein (CHOP), and Poly (ADP-ribose) polymerase-1 (PARP-1) (Schauvliege et al., 2002; Endo et al., 2006; Yoo et al., 2011). The only identified transcription factor known to control CASP11 expression following IFN $\gamma$  priming is STAT1 (Schauvliege et al., 2002). Future research that expands our understanding of the transcription factors regulating CASP11 expression under different priming conditions may help to clarify the functional differences we observe between these conditions.

The effects of IFN $\gamma$  treatment on macrophages are pleiotropic but generally understood to drive antimicrobial responses (Schroder et al., 2004). Hundreds of genes are transcriptionally induced, rates of mRNA translation are shifted, and changes to metabolism highlight just some of the changes that occur following IFN $\gamma$  treatment (Su et al., 2015). Thus, the phenotype described in this manuscript could be regulated transcriptionally, translationally, or enzymatically. The pleiotropic effects of IFN $\gamma$  treatment are akin to our understanding of IFN-driven mechanisms that are broadly antiviral. For example, hundreds of interferon stimulated genes (ISGs) contribute to antiviral mechanisms that protect the host, yet our understanding of their functional relevance individually remains limited (Schoggins, 2019).

As mentioned previously, a strength of our study is derived from the comparison between different priming agents on inflammasome outcome. The greatest difference in response was observed between IFN $\gamma$  and LPS priming, which could not be explained by differential CASP11 or GBP expression. Our interpretation of these results led us to hypothesize that IFN $\gamma$  priming may induce the expression or activity of an enhancer(s) that promotes CASP11 inflammasome activation. Alternatively, LPS may induce the expression or activity of a negative regulator(s) that inhibits CASP11 inflammasome activation. This alternative hypothesis would fit with most of the data that we present in this manuscript. However, experiments utilizing the constitutive CASP11 expressing cell line suggest this may not be the case. Specifically, LPS priming in this cell line promoted higher levels of cell death following CASP11 activation compared with unprimed cells (Figure 3C). If LPS priming induced the expression or activity of an inhibitor, we might expect to see lower levels of CASP11-induced cell death in this cell line as compared with unprimed cells.

Future studies are required to test these hypotheses and may lead to the identification of our proposed IFN $\gamma$ -inducible enhancer(s) of CASP11 activation or an LPS-inducible inhibitor(s) of the same response. We speculate that unknown CASP11 regulators that either enhance or inhibit the response to cytosolic LPS may also play a role in CASP4/CASP5-dependent responses in human cells. Furthermore, the identification of unknown enhancers or inhibitors to these responses may aid in drug development for treating bacterial infections or sepsis.

### Limitations of the Study

Several publications have highlighted inflammasome activation differences between mouse and human systems. Our study was limited to experiments in mouse macrophages, which provided us with the specific advantage of utilizing primary cells (BMDMs) for the majority of our experiments. Therefore, it will be of importance to compare different priming agents in the context of human CASP4/CASP5 inflammasome activation. Given that CASP4 is constitutively expressed in many cell types, inducible regulators of the response to cytosolic LPS may be even more important in this context. Additionally, it was beyond the scope of this manuscript to compare priming conditions in other cell types. It will be interesting to determine if IFN $\gamma$  priming enhances CASP11 inflammasome activation in other cell types or if this response is specific to macrophages.

### Resource Availability

#### Lead Contact

Further information and requests for resources and reagents should be directed to and will be fulfilled by Denise Monack ([dmonack@stanford.edu](mailto:dmonack@stanford.edu)).

#### Materials Availability

All unique/stable reagents generated in this study are available from the Lead Contact without restriction.

#### Data and Code Availability

The dataset supporting the current study is available from the lead contact upon reasonable request.

## METHODS

All methods can be found in the accompanying [Transparent Methods supplemental file](#).

## SUPPLEMENTAL INFORMATION

Supplemental Information can be found online at <https://doi.org/10.1016/j.isci.2020.101612>.

## ACKNOWLEDGMENTS

The authors thank Manuel Amieva as well as members of the Monack and Amieva laboratories for valuable discussion and technical support. The following funding sources supported the research reported in this manuscript: NIAID, United States 1R01 AI109539, NIAID, United States 2R01 AI095396-06, NIGMS, United States T32GM007276, NIAID, United States 5T32AI00729035, Dean's Postdoctoral Fellowship—Stanford School of Medicine, Stanford Graduate Fellowship—Gabilan Fellow, Allen Stanford Discovery Center Grant to D.M.M. from the Paul Allen Family Foundation. The graphical abstract was created with [BioRender.com](https://BioRender.com).



## AUTHOR CONTRIBUTIONS

Conceptualization, S.W.B. and D.M.M.; Investigation S.W.B., S.M.B., and L.M.M.; B.A.N. made *Casp1*-*Casp11*-CRISPR/Cas9 DKO RAW macrophages utilized in this study; Writing – Original Draft, S.W.B.; Writing – Review & Editing, S.W.B., S.M.B., and D.M.M.; Funding Acquisition, S.W.B., S.M.B., and D.M.M.

## DECLARATION OF INTERESTS

The authors declare no competing interests.

Received: January 30, 2020

Revised: August 25, 2020

Accepted: September 22, 2020

Published: October 23, 2020

## REFERENCES

- Aachoui, Y., Kajiwara, Y., Leaf, I.A., Mao, D., Ting, J.P., Coers, J., Aderem, A., Buxbaum, J.D., and Miao, E.A. (2015). Canonical inflammasomes drive IFN-gamma to Prime Caspase-11 in defense against a cytosol-invasive bacterium. *Cell Host Microbe* 18, 320–332.
- Aachoui, Y., Leaf, I.A., Hagar, J.A., Fontana, M.F., Campos, C.G., Zak, D.E., Tan, M.H., Cotter, P.A., Vance, R.E., Aderem, A., and Miao, E.A. (2013). Caspase-11 protects against bacteria that escape the vacuole. *Science* 339, 975–978.
- Aglietti, R.A., Estevez, A., Gupta, A., Ramirez, M.G., Liu, P.S., Kayagaki, N., Ciferri, C., Dixit, V.M., and Dueber, E.C. (2016). GsdmD p30 elicited by caspase-11 during pyroptosis forms pores in membranes. *Proc. Natl. Acad. Sci. U S A* 113, 7858–7863.
- Aizawa, E., Karasawa, T., Watanabe, S., Komada, T., Kimura, H., Kamata, R., Ito, H., Hishida, E., Yamada, N., Kasahara, T., et al. (2020). GSDME-dependent incomplete pyroptosis permits selective IL-1alpha release under caspase-1 inhibition. *iScience* 23, 101070.
- Akira, S., and Takeda, K. (2004). Toll-like receptor signalling. *Nat. Rev. Immunol.* 4, 499–511.
- Bauernfeind, F., Niepmann, S., Knolle, P.A., and Hornung, V. (2016). Aging-associated TNF production primes inflammasome activation and NLRP3-related metabolic disturbances. *J. Immunol.* 197, 2900–2908.
- Bauernfeind, F.G., Horvath, G., Stutz, A., Alnemri, E.S., Macdonald, K., Speert, D., Fernandes-Alnemri, T., Wu, J., Monks, B.G., Fitzgerald, K.A., et al. (2009). Cutting edge: NF-kappaB activating pattern recognition and cytokine receptors license NLRP3 inflammasome activation by regulating NLRP3 expression. *J. Immunol.* 183, 787–791.
- Broz, P., Ruby, T., Belhocine, K., Bouley, D.M., Kayagaki, N., Dixit, V.M., and Monack, D.M. (2012). Caspase-11 increases susceptibility to Salmonella infection in the absence of caspase-1. *Nature* 490, 288–291.
- Brubaker, S.W., Bonham, K.S., Zanoni, I., and Kagan, J.C. (2015). Innate immune pattern recognition: a cell biological perspective. *Annu. Rev. Immunol.* 33, 257–290.
- Brubaker, S.W., Gauthier, A.E., Mills, E.W., Ingolia, N.T., and Kagan, J.C. (2014). A bicistronic MAVS transcript highlights a class of truncated variants in antiviral immunity. *Cell* 156, 800–811.
- Cerqueira, D.M., Gomes, M.T.R., Silva, A.L.N., Rungue, M., Assis, N.R.G., Guimaraes, E.S., Morais, S.B., Broz, P., Zamboni, D.S., and Oliveira, S.C. (2018). Guanylate-binding protein 5 licenses caspase-11 for gasdermin-D mediated host resistance to brucella abortus infection. *PLoS Pathog.* 14, e1007519.
- Chen, K.W., Demarco, B., Heilig, R., Shkarina, K., Boettcher, A., Farady, C.J., Pelczar, P., and Broz, P. (2019). Extrinsic and intrinsic apoptosis activate pannexin-1 to drive NLRP3 inflammasome assembly. *EMBO J.* 38, e101638.
- Ding, J., Wang, K., Liu, W., She, Y., Sun, Q., Shi, J., Sun, H., Wang, D.C., and Shao, F. (2016). Pore-forming activity and structural autoinhibition of the gasdermin family. *Nature* 535, 111–116.
- Endo, M., Mori, M., Akira, S., and Gotoh, T. (2006). C/EBP homologous protein (CHOP) is crucial for the induction of caspase-11 and the pathogenesis of lipopolysaccharide-induced inflammation. *J. Immunol.* 176, 6245–6253.
- Finethy, R., Jorgensen, I., Haldar, A.K., De Zoete, M.R., Strowig, T., Flavell, R.A., Yamamoto, M., Nagarajan, U.M., Miao, E.A., and Coers, J. (2015). Guanylate binding proteins enable rapid activation of canonical and noncanonical inflammasomes in chlamydia-infected macrophages. *Infect. Immun.* 83, 4740–4749.
- Finethy, R., Luoma, S., Orench-Rivera, N., Feeley, E.M., Haldar, A.K., Yamamoto, M., Kanneganti, T.D., Kuehn, M.J., and Coers, J. (2017). Inflammasome activation by bacterial outer membrane vesicles requires guanylate binding proteins. *mBio* 8, e01188-17.
- Fisch, D., Bando, H., Clough, B., Hornung, V., Yamamoto, M., Shenoy, A.R., and Frickel, E.M. (2019). Human GBP1 is a microbe-specific gatekeeper of macrophage apoptosis and pyroptosis. *EMBO J.* 38, e100926.
- Gu, L., Meng, R., Tang, Y., Zhao, K., Liang, F., Zhang, R., Xue, Q., Chen, F., Xiao, X., Wang, H., et al. (2019). Toll-like receptor 4 signaling licenses the cytosolic transport of lipopolysaccharide from bacterial outer membrane vesicles. *Shock* 51, 256–265.
- Hagar, J.A., Powell, D.A., Aachoui, Y., Ernst, R.K., and Miao, E.A. (2013). Cytoplasmic LPS activates caspase-11: implications in TLR4-independent endotoxic shock. *Science* 341, 1250–1253.
- Huang, S., Hendriks, W., Althage, A., Hemmi, S., Bluethmann, H., Kamijo, R., Vilcek, J., Zinkernagel, R.M., and Aguet, M. (1993). Immune response in mice that lack the interferon-gamma receptor. *Science* 259, 1742–1745.
- Kang, S.J., Wang, S., Hara, H., Peterson, E.P., Namura, S., Amin-Hanjani, S., Huang, Z., Srinivasan, A., Tomaselli, K.J., Thornberry, N.A., et al. (2000). Dual role of caspase-11 in mediating activation of caspase-1 and caspase-3 under pathological conditions. *J. Cell Biol.* 149, 613–622.
- Kayagaki, N., Lee, B.L., Stowe, I.B., Kornfeld, O.S., O'Rourke, K., Mirrashidi, K.M., Haley, B., Watanabe, C., Roose-Girma, M., Modrusan, Z., et al. (2019). IRF2 transcriptionally induces GSDMD expression for pyroptosis. *Sci. Signal.* 12, eaax4917.
- Kayagaki, N., Stowe, I.B., Lee, B.L., O'Rourke, K., Anderson, K., Warming, S., Cuellar, T., Haley, B., Roose-Girma, M., Phung, Q.T., et al. (2015). Caspase-11 cleaves gasdermin D for non-canonical inflammasome signalling. *Nature* 526, 666–671.
- Kayagaki, N., Warming, S., Lamkanfi, M., Vande Walle, L., Louie, S., Dong, J., Newton, K., Qu, Y., Liu, J., Heldens, S., et al. (2011). Non-canonical inflammasome activation targets caspase-11. *Nature* 479, 117–121.
- Kayagaki, N., Wong, M.T., Stowe, I.B., Ramani, S.R., Gonzalez, L.C., Akashi-Takamura, S., Miyake, K., Zhang, J., Lee, W.P., Muszynski, A., et al. (2013). Noncanonical inflammasome activation by intracellular LPS independent of TLR4. *Science* 341, 1246–1249.
- Kovacs, S.B., Oh, C., Maltez, V.I., Mcglaughon, B.D., Verma, A., Miao, E.A., and Aachoui, Y. (2020). Neutrophil caspase-11 is essential to defend against a cytosol-invasive bacterium. *Cell Rep* 32, 107967.
- Latz, E., Xiao, T.S., and Stutz, A. (2013). Activation and regulation of the inflammasomes. *Nat. Rev. Immunol.* 13, 397–411.

- Li, W., Xu, H., Xiao, T., Cong, L., Love, M.I., Zhang, F., Irizarry, R.A., Liu, J.S., Brown, M., and Liu, X.S. (2014). MAGeCK enables robust identification of essential genes from genome-scale CRISPR/Cas9 knockout screens. *Genome Biol.* 15, 554.
- Liu, X., Zhang, Z., Ruan, J., Pan, Y., Magupalli, V.G., Wu, H., and Lieberman, J. (2016). Inflammasome-activated gasdermin D causes pyroptosis by forming membrane pores. *Nature* 535, 153–158.
- Man, S.M., Karki, R., Sasai, M., Place, D.E., Kesavardhana, S., Temirov, J., Frase, S., Zhu, Q., Malireddi, R.K.S., Kuriakose, T., et al. (2016). IRG1 liberates bacterial ligands for sensing by the AIM2 and caspase-11-NLRP3 inflammasomes. *Cell* 167, 382–396 e17.
- Meunier, E., Dick, M.S., Dreier, R.F., Schurmann, N., Kenzelmann Broz, D., Warming, S., Roose-Girma, M., Bumann, D., Kayagaki, N., Takeda, K., et al. (2014). Caspase-11 activation requires lysis of pathogen-containing vacuoles by IFN-induced GTPases. *Nature* 509, 366–370.
- Meunier, E., Wallet, P., Dreier, R.F., Costanzo, S., Anton, L., Ruhl, S., Dussurgey, S., Dick, M.S., Kistner, A., Rigard, M., et al. (2015). Guanylate-binding proteins promote activation of the AIM2 inflammasome during infection with *Francisella novicida*. *Nat. Immunol.* 16, 476–484.
- Orning, P., Weng, D., Starheim, K., Ratner, D., Best, Z., Lee, B., Brooks, A., Xia, S., Wu, H., Kelliher, M.A., et al. (2018). Pathogen blockade of TAK1 triggers caspase-8-dependent cleavage of gasdermin D and cell death. *Science* 362, 1064–1069.
- Pilla, D.M., Hagar, J.A., Haldar, A.K., Mason, A.K., Degrandi, D., Pfeffer, K., Ernst, R.K., Yamamoto, M., Miao, E.A., and Coers, J. (2014). Guanylate binding proteins promote caspase-11-dependent pyroptosis in response to cytoplasmic LPS. *Proc. Natl. Acad. Sci. U S A* 111, 6046–6051.
- Rathinam, V.A., Vanaja, S.K., Waggoner, L., Sokolovska, A., Becker, C., Stuart, L.M., Leong, J.M., and Fitzgerald, K.A. (2012). TRIF licenses caspase-11-dependent NLRP3 inflammasome activation by gram-negative bacteria. *Cell* 150, 606–619.
- Rogers, C., Fernandes-Alnemri, T., Mayes, L., Alnemri, D., Cingolani, G., and Alnemri, E.S. (2017). Cleavage of DFNA5 by caspase-3 during apoptosis mediates progression to secondary necrotic/pyroptotic cell death. *Nat. Commun.* 8, 14128.
- Ruhl, S., and Broz, P. (2015). Caspase-11 activates a canonical NLRP3 inflammasome by promoting K(+) efflux. *Eur. J. Immunol.* 45, 2927–2936.
- Sagulenko, V., Thygesen, S.J., Sester, D.P., Idris, A., Cridland, J.A., Vajjhala, P.R., Roberts, T.L., Schroder, K., Vince, J.E., Hill, J.M., et al. (2013). AIM2 and NLRP3 inflammasomes activate both apoptotic and pyroptotic death pathways via ASC. *Cell Death Differ.* 20, 1149–1160.
- Sanjana, N.E., Shalem, O., and Zhang, F. (2014). Improved vectors and genome-wide libraries for CRISPR screening. *Nat. Methods* 11, 783–784.
- Santos, J.C., Boucher, D., Schneider, L.K., Demarco, B., Dilucca, M., Shkarina, K., Heilig, R., Chen, K.W., Lim, R.Y.H., and Broz, P. (2020). Human GBP1 binds LPS to initiate assembly of a caspase-4 activating platform on cytosolic bacteria. *Nat. Commun.* 11, 3276.
- Santos, J.C., Dick, M.S., Lagrange, B., Degrandi, D., Pfeffer, K., Yamamoto, M., Meunier, E., Pelczar, P., Henry, T., and Broz, P. (2018). LPS targets host guanylate-binding proteins to the bacterial outer membrane for non-canonical inflammasome activation. *EMBO J.* 37, e98089.
- Sarhan, J., Liu, B.C., Muendlein, H.I., Li, P., Nilson, R., Tang, A.Y., Rongvaux, A., Bunnell, S.C., Shao, F., Green, D.R., and Poltorak, A. (2018). Caspase-8 induces cleavage of gasdermin D to elicit pyroptosis during *Yersinia* infection. *Proc. Natl. Acad. Sci. U S A* 115, E10888–E10897.
- Schauvliege, R., Vanrobaeys, J., Schotte, P., and Beyaert, R. (2002). Caspase-11 gene expression in response to lipopolysaccharide and interferon-gamma requires nuclear factor-kappa B and signal transducer and activator of transcription (STAT) 1. *J. Biol. Chem.* 277, 41624–41630.
- Schneider, K.S., Gross, C.J., Dreier, R.F., Saller, B.S., Mishra, R., Gorka, O., Heilig, R., Meunier, E., Dick, M.S., Cikovic, T., et al. (2017). The inflammasome drives GSDMD-independent secondary pyroptosis and IL-1 release in the absence of caspase-1 protease activity. *Cell Rep.* 21, 3846–3859.
- Schoggins, J.W. (2019). Interferon-stimulated genes: what do they all do? *Annu. Rev. Virol.* 6, 567–584.
- Schroder, K., Hertzog, P.J., Ravasi, T., and Hume, D.A. (2004). Interferon-gamma: an overview of signals, mechanisms and functions. *J. Leukoc. Biol.* 75, 163–189.
- Shi, J., Zhao, Y., Wang, K., Shi, X., Wang, Y., Huang, H., Zhuang, Y., Cai, T., Wang, F., and Shao, F. (2015). Cleavage of GSDMD by inflammatory caspases determines pyroptotic cell death. *Nature* 526, 660–665.
- Shi, J., Zhao, Y., Wang, Y., Gao, W., Ding, J., Li, P., Hu, L., and Shao, F. (2014). Inflammatory caspases are innate immune receptors for intracellular LPS. *Nature* 514, 187–192.
- Su, X., Yu, Y., Zhong, Y., Giannopoulou, E.G., Hu, X., Liu, H., Cross, J.R., Ratsch, G., Rice, C.M., and Ivashkiv, L.B. (2015). Interferon-gamma regulates cellular metabolism and mRNA translation to potentiate macrophage activation. *Nat. Immunol.* 16, 838–849.
- Tang, Y., Zhang, R., Xue, Q., Meng, R., Wang, X., Yang, Y., Xie, L., Xiao, X., Billiar, T.R., and Lu, B. (2018). TRIF signaling is required for caspase-11-dependent immune responses and lethality in sepsis. *Mol. Med.* 24, 66.
- Tretina, K., Park, E.S., Maminska, A., and Macmicking, J.D. (2019). Interferon-induced guanylate-binding proteins: guardians of host defense in health and disease. *J. Exp. Med.* 216, 482–500.
- Wandel, M.P., Kim, B.H., Park, E.S., Boyle, K.B., Nayak, K., Lagrange, B., Herod, A., Henry, T., Zilbauer, M., Rohde, J., et al. (2020). Guanylate-binding proteins convert cytosolic bacteria into caspase-4 signaling platforms. *Nat. Immunol.* 21, 880–891.
- Wang, Y., Gao, W., Shi, X., Ding, J., Liu, W., He, H., Wang, K., and Shao, F. (2017). Chemotherapy drugs induce pyroptosis through caspase-3 cleavage of a gasdermin. *Nature* 547, 99–103.
- Yamamoto, M., Okuyama, M., Ma, J.S., Kimura, T., Kamiyama, N., Saiga, H., Ohshima, J., Sasai, M., Kayama, H., Okamoto, T., et al. (2012). A cluster of interferon-gamma-inducible p65 GTPases plays a critical role in host defense against *Toxoplasma gondii*. *Immunity* 37, 302–313.
- Yoo, L., Hong, S., Shin, K.S., and Kang, S.J. (2011). PARP-1 regulates the expression of caspase-11. *Biochem. Biophys. Res. Commun.* 408, 489–493.

iScience, Volume 23

## **Supplemental Information**

### **A Rapid Caspase-11 Response Induced by IFN $\gamma$ Priming Is Independent of Guanylate Binding Proteins**

**Sky W. Brubaker, Susan M. Brewer, Liliana M. Massis, Brooke A. Napier, and Denise M. Monack**

Figure S1

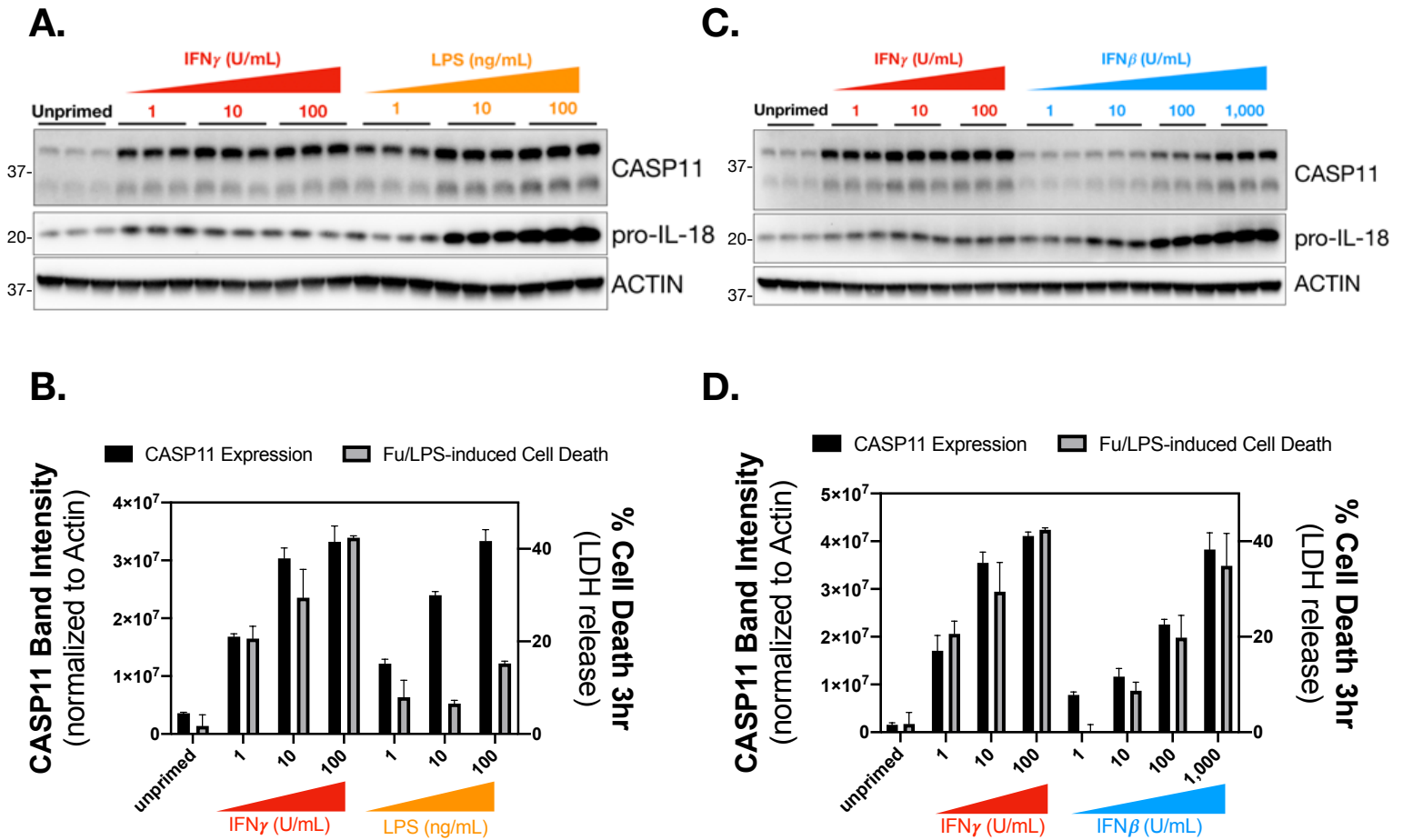


**Figure S1. IFN $\gamma$  is a More Potent Priming Agent for CASP11-dependent inflammasome activation. Related to Figure 1**

WT BMDMs were primed as indicated for 16hrs overnight in technical triplicate and cell lysates were collected to determine the expression levels of CASP11 and pro-IL-18 by Western blot (A,C). In parallel, WT BMDMs were primed as indicated for CASP11 activation by LPS (*E. coli* 0111:B4, 25ug/mL) transfection with FugeneHD (Fu/LPS). At 3hrs following inflammasome activation, supernatants were collected to measure release of LDH for percent cell death calculations. Quantitations of CASP11 expression (from A,C) are compared against Fu/LPS-induced cell death (B,D). Bar graphs in black correspond to the left axis, which represents CASP11 expression as band intensity normalized to ACTIN. Percent cell death at 3 hours following LPS transfection is plotted in grey and corresponds to the right axis. Bar graphs depict the mean +/- SD using triplicates for each condition. Molecular weight marker positions are shown to the left of each blot. Data are representative of 4 (A,B) or 3 (C,D) independent experiments.

## Figure S2

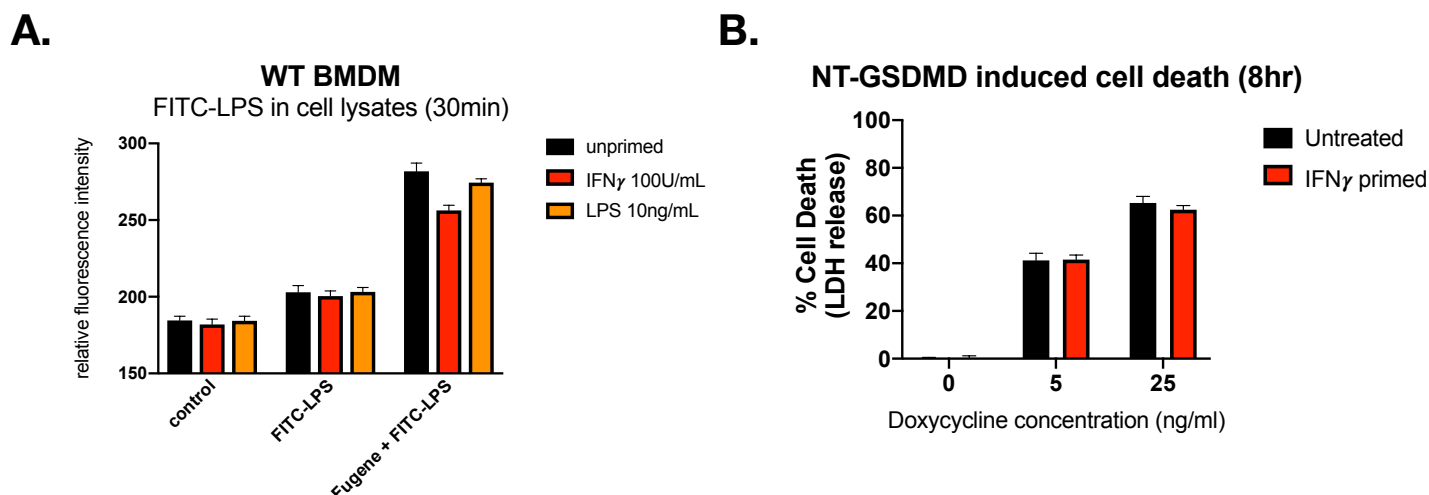


**Figure S2. IFN $\gamma$  Priming Does not Promote Transfection-dependent Delivery of LPS or NT-GSDMD Pore Formation. Related to Figure 2**

(A) Transfection-dependent delivery of LPS was determined using a FITC-labelled LPS conjugate. WT BMDMs were primed for 16hrs overnight with the following treatments; unprimed (N/A), IFN $\gamma$  (100U/mL), or LPS (10ng/mL). The BMDMs were then transfected with a FITC-conjugated LPS (*E. coli* 0111:B4, 25ug/mL) using FugeneHD. Following transfection, cell lysates were collected, and the relative fluorescence intensity of lysates was measured. (B) A Doxycycline-inducible NT-GSDMD cell line was generated in *Gsdmd*-CRISPR/Cas9 KO RAW cells. Prior to Dox-induced expression of NT-GSDMD, cells were treated with or without IFN $\gamma$  (100U/mL) for 16hrs. Following Dox-induced expression of NT-GSDMD, cell death was determined by measuring release of LDH in the supernatant. Bar graphs show the mean value  $\pm$  SD of triplicates (A,B). Data are representative of 2 independent experiments (A,B).

Figure S3

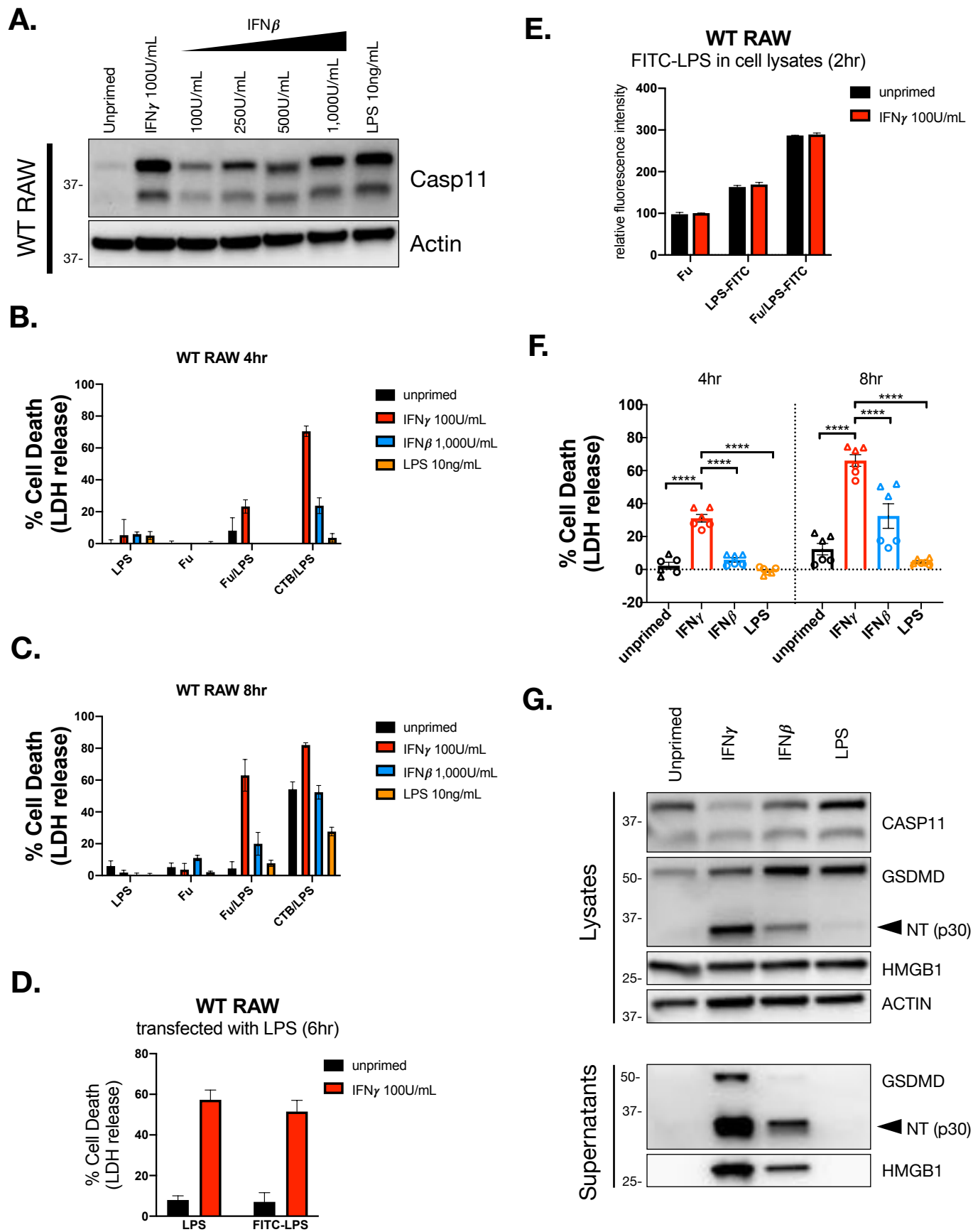


**Figure S3. IFN $\gamma$  Priming Enhances CASP11-dependent Cell Death in RAW 264.7 Independently of CASP11 Expression. Related to Figure 3**

(A) WT RAW 264.7 cells were left unprimed or treated with IFN $\gamma$ , IFN $\beta$ , or LPS at the indicated concentrations for 16hrs and cell lysates were collected to determine the expression of CASP11 by Western blot. (B-C) WT RAW 264.7 cells were primed for 16hrs overnight with the following treatments: unprimed (N/A), IFN $\gamma$  (100U/mL), IFN $\beta$  (1,000U/mL), or LPS (10ng/mL). Cells were treated with LPS (*E. coli* 0111:B4, 25ug/mL), FugeneHD (0.5%), LPS and FugeneHD, or LPS with CTB (Cholera Toxin B Subunit, 20ug/mL). At 4hrs (B) and 8hrs (C) following inflammasome activation, supernatants were collected to measure release of LDH for percent cell death calculations. (D) WT RAW 264.7 cells were left unprimed or treated with IFN $\gamma$  (100U/mL) for 16hrs and CASP11 inflammasome activation was triggered by FITC-conjugated or standard LPS (*E. coli* 0111:B4, 25ug/mL) transfection using FugeneHD. Supernatants were collected to measure release of LDH for percent cell death calculations. (E) Transfection-dependent delivery of LPS was determined using the FITC-labeled LPS conjugate. WT RAW 264.7 cells were primed with or without IFN $\gamma$  (100U/mL) for 16hrs and FITC-LPS was transfected with FugeneHD. Following transfection, cell lysates were collected, and the relative fluorescence intensity of lysates was measured. (F-G) The constitutive CASP11-expressing cell line was primed for 16hrs overnight with the following treatments: unprimed (N/A), IFN $\gamma$  (100U/mL), IFN $\beta$  (1,000U/mL), or LPS (10ng/mL). CASP11 inflammasome activation was triggered with a mixture of LPS (*E. coli* 0111:B4, 50ug/mL) and CTB (20ug/mL). (F) At 4 and 8hrs following inflammasome activation, supernatants were collected to measure release of LDH for percent cell death calculations. (G) Alternatively, supernatants and lysates were collected 6hrs post-transfection to monitor for the cleavage and release of inflammasome-related proteins by SDS-PAGE and Western blot. Molecular weight marker positions are shown to the left of each blot, and arrows indicate a cleavage product. Bar graphs (B-E) show the mean value +/- SD of technical triplicates and are representative of at least 2 independent experiments. Bar graphs (F) show the mean value +/- SEM along with individual data points pooled from 2 independent experiments depicted with different shapes. Western blots (A,G) are representative of 2 independent experiments. Statistical analysis performed using a Two-way ANOVA and Tukey's multiple comparisons test; \*\*\*\* < 0.0001

Figure S4

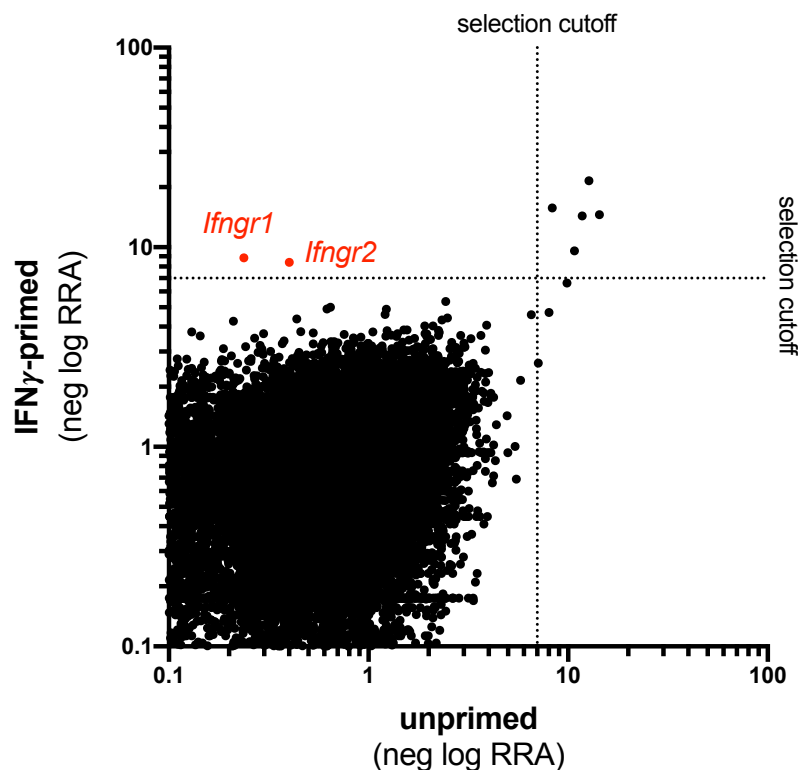


**Figure S4. Genome-wide CRISPR KO Survival Screen Identifies Genes Encoding IFN $\gamma$  Receptor. Related to Figure 4**

We generated a genome-wide CRISPR knockout library in the constitutive CASP11 expressing cells (described in Figure 3) and selected for surviving cell populations following treatment with or without IFN $\gamma$  priming and transfected with LPS. Each axis depicts the enrichment score for gRNAs present in the surviving population calculated using MAGeCK and an arbitrary selection cutoff was made at a negative log RRA enrichment score of 7. Cell populations with gRNAs targeting *Ifngr1* and *Ifngr2* (highlighted in red) were only selected following Casp11 activation with IFN $\gamma$  priming (y-axis) compared with an unprimed selection (x-axis).



Figure S5

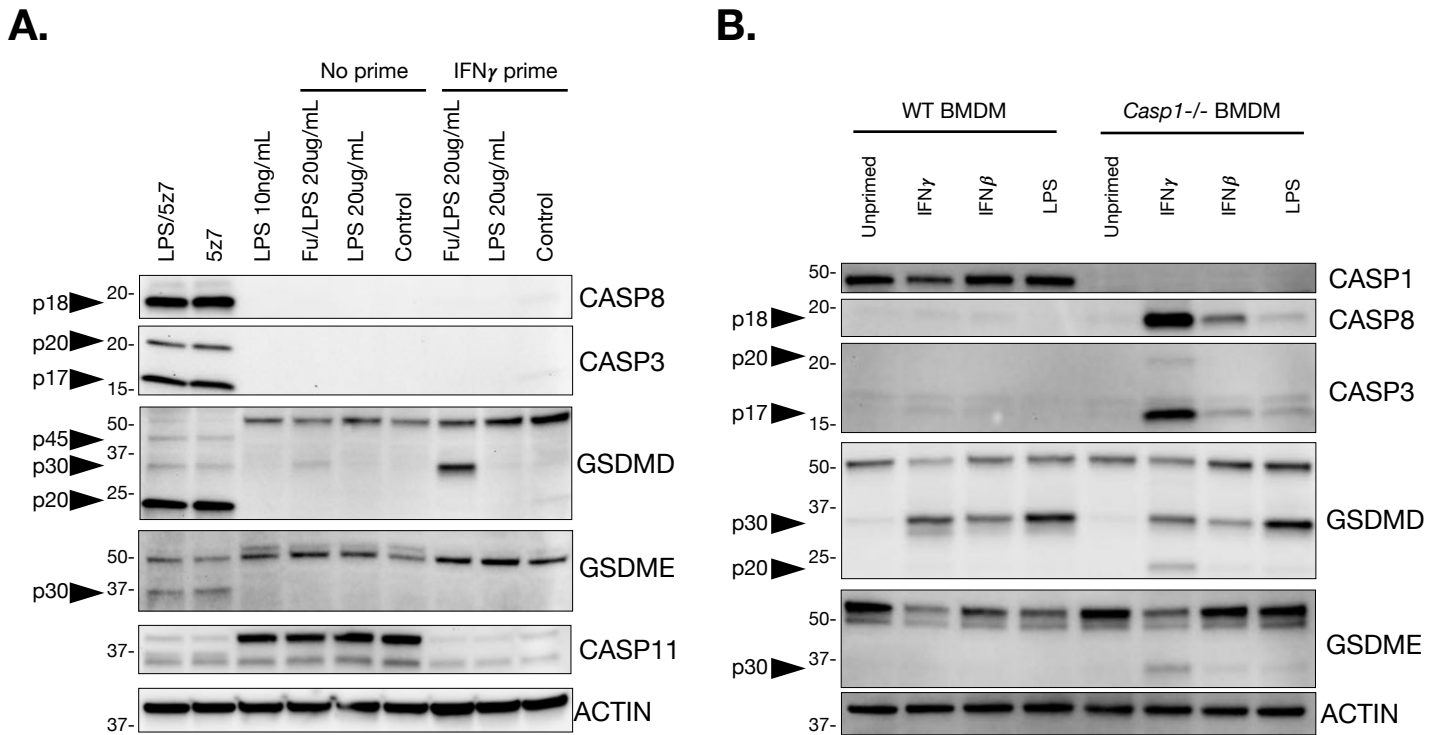
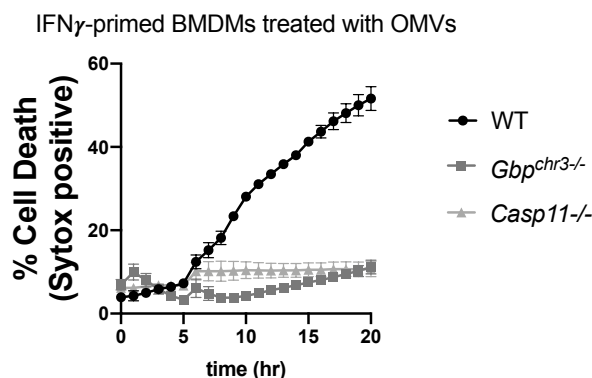


**Figure S5. IFN $\gamma$  Enhancement of CASP11-dependent Cell Death is not Associated with GSDME Cleavage. Related to Figure 5**

(A) Constitutive CASP11-expressing RAW cells (see Figure 3) were primed +/- IFN $\gamma$  for 16hrs and CASP11 activation was triggered by LPS (*E. coli* 0111:B4, 25ug/mL) transfection with EugeneHD. Following transfection (7hrs) cell lysates and supernatants were collected and pooled to determine Caspase and Gasdermin cleavage by Western blot. As a positive control for CASP8, CASP3, and GSDME cleavage, cells were treated with the TAK1 inhibitor 5z7. (B) WT and *Casp1*<sup>-/-</sup> BMDMs were treated with the indicated priming agents for 16hrs and transfected with LPS (*E. coli* 0111:B4, 25ug/mL). Following transfection, cell lysates were collected at 3hrs and analyzed by Western blot to determine Caspase and Gasdermin cleavage. Molecular weight marker positions are shown to the left of each blot, and arrows indicate a cleavage product. Data represent results from single experiments (A-B).

## Figure S6

A.



B.

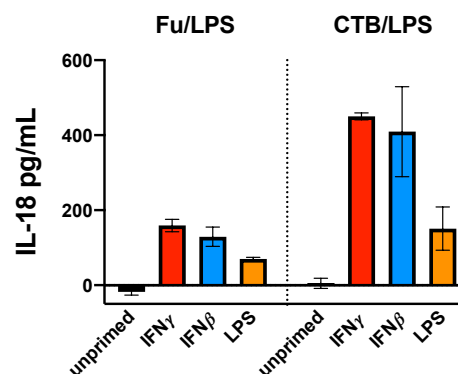


**Figure S6. IFN-Inducible GBPs do not Fully Account for Enhanced CASP11-dependent Cell Death Triggered by IFN $\gamma$  Priming. Related to Figure 6**

(A) WT, *Gbpchr3*<sup>-/-</sup>, and *Casp11*<sup>-/-</sup> BMDMs were primed for 16hrs overnight with IFN $\gamma$  (100U/mL) and CASP11 inflammasome activation was triggered by treating cells with OMVs (*E. coli* DH5 $\alpha$ ). Cell death kinetics were monitored over time by measuring the incorporation of SYTOX Green. (B) *Gbpchr3*<sup>-/-</sup> BMDMs were primed for 16hrs overnight with the following treatments: unprimed (N/A), IFN $\gamma$  (100U/mL), IFN $\beta$  (100U/mL), LPS (10ng/mL). CASP11 inflammasome activation was triggered by LPS (*E. coli* 0111:B4, 25ug/mL) transfection with FugeneHD, or LPS (*E. coli* 0111:B4, 25ug/mL) mixed with CTB (Cholera Toxin B Subunit, 20ug/mL). At 3hrs following inflammasome activation, supernatants were collected to measure release of IL-18. Line graph shows the mean value  $\pm$  SEM pooled from 2 independent experiments with technical replicates (A). Bar graph shows the mean value  $\pm$  SD of samples in triplicate from one experiment (B).

1 **Transparent Methods:**

2 Experimental Models

3 *Cell lines and primary cell cultures:*

4 Primary BMDMs were differentiated from flushed femurs as described previously  
5 (Broz and Monack 2013). All animal care and the bone marrow isolation procedures  
6 used in this study for differentiating BMDMs were approved and are in accordance with  
7 the guidelines set out by Stanford University's Administrative Panel on Laboratory  
8 Animal Care (APLAC). Briefly 6-14 week old mice were euthanized and following bone  
9 marrow, isolation cells were cultured in differentiation media: Dulbecco's Modified Eagle  
10 Media (DMEM) containing L-Glutamine 4mM, D-Glucose 25mM, Sodium Pyruvate 1mM  
11 (ThermoFisher catalogue #11995073) supplemented with 10% Fetal Bovine Serum  
12 (FBS) and 20% conditioned media from MCSF-producing 3T3 cells (provided by Anita  
13 Sil UCSF). Differentiation was conducted over 6 days in non-"TC treated" culture plates,  
14 BMDMs were lifted by gentle scraping in ice-cold PBS, and frozen down in cryovials at  
15  $1 \times 10^7$  cells/mL in FBS containing 10% DMSO. MCSF conditioned media from 3T3 cells  
16 was generated by splitting a confluent flask of MCSF-producing 3T3 cells 1:10 in DMEM  
17 containing L-Glutamine 4mM, D-Glucose 25mM, Sodium Pyruvate 1mM (ThermoFisher  
18 catalogue #11995073) supplemented with 10% FBS. Supernatants were collected on  
19 day four and the media was replenished for a second collection on day seven. MCSF  
20 conditioned media from day four and seven were pooled, filter sterilized (0.2  $\mu$ m filter  
21 flask), and stored at -80°C. Both male and female mice were used for BMDM  
22 differentiation. We have not observed inflammasome activation differences *in vitro*

23 between BMDMs isolated from male or female mice. WT C57BL/6NJ (Stock No.  
24 005304) and *Ifngr1*<sup>-/-</sup> (Stock No. 003288) mice were acquired from Jackson Labs,  
25 femurs and/or bone marrow from knockout mice were provided by Vishva Dixit  
26 (*Casp11*<sup>-/-</sup>, *Casp1*<sup>-/-</sup>, *Gsdmd*<sup>-/-</sup>, and *Gsdme*<sup>-/-</sup>), Petr Broz and Igor Brodsky (*Gbp*<sup>chr3-/-</sup>).

27 RAW 264.7 macrophages are an Abelson murine leukemia virus transformed cell  
28 line derived from male mice and were obtained from ATCC (TIB-71). RAW cells were  
29 cultured in DMEM containing L-Glutamine 4mM, D-Glucose 25mM, Sodium Pyruvate  
30 1mM (ThermoFisher catalogue #11995073) supplemented with 10% FBS.

31

32 *Method Details:*

33 Macrophage treatments:

34 Macrophages were seeded into 96-well (40,000 cells/well) or 6-well (1x10<sup>6</sup>  
35 cells/well) plates with macrophage media: DMEM, containing L-Glutamine 4mM, D-  
36 Glucose 25mM, Sodium Pyruvate 1mM (ThermoFisher catalogue #11995073)  
37 supplemented with 10% Fetal Bovine Serum (FBS) and 10% conditioned media from  
38 MCSF-producing 3T3 cells (see above). Once macrophages adhered to the plate, cells  
39 were primed (16hr) with the indicated priming agents by adding a 1:1 volume of a 2x  
40 working stock diluted in bone marrow macrophage media. In our hands, transfection  
41 efficiency is improved with the use of Opti-MEM media and LDH assays are more  
42 robust with media that does not contain Phenol red. Therefore, all inflammasome  
43 activation assays were carried out in Phenol red-free Opti-MEM (Gibco #11058021 and  
44 referred to as Opti-MEM throughout) to match the optimized conditions for LPS

45 transfection. Prior to transfection (LPS) or treatment (Nigericin, ATP, CTB/LPS, OMV),  
46 macrophage media in the plate was removed and replaced with Opti-MEM. For LPS  
47 transfection in BMDMs and WT RAW 264.7 macrophages, LPS (*E. coli* 0111:B4;  
48 Invivogen LPS-EB VacciGrade Cat #vac-3pelps; 20-25ug/mL final concentration) and  
49 FuGENE HD (0.5-0.6% final concentration) were complexed in Opti-MEM by briefly  
50 vortexing and allowing the solution to incubate for 15-30min at room temperature. The  
51 LPS/FuGENE HD complex was then overlayed in each well containing Opti-MEM. For  
52 transfection in *Casp1, Casp11*-DKO +*Casp11* RAW cells, the same amounts of LPS and  
53 FuGENE HD were used, however the final volume of Opti-MEM was reduced by half to  
54 increase transfection efficiency. For NLRP3 inflammasome activation, ATP (5mM final  
55 concentration) or Nigericin (10uM final concentration) were prepared in Opti-MEM and  
56 added to macrophages in Opti-MEM. For CTB/LPS treatments, LPS (20-25ug/mL final  
57 concentration) and CTB (List Biological Laboratories #104; 20ug/mL final concentration)  
58 were mixed in Opti-MEM by pipetting up and down and allowed to incubate for 15-  
59 30min at room temperature. The CTB/LPS complex was then overlayed on  
60 macrophages in wells containing Opti-MEM. For OMV treatments, *E. coli* derived OMVs  
61 (10uL/well 96well) resuspended in PBS were added to BMDMs in Opti-MEM (see more  
62 on OMV isolation below). As a positive control to activate CASP8/CASP3/Gsdme, cells  
63 were treated with the TAK1 inhibitor (5z7) as described previously (Sarhan et al).  
64 Briefly, 5z7 (125nM) with or without LPS (10ng/mL) in serum-free media was added to  
65 cells for 5hr. Proteins in the supernatant were precipitated with TCA and combined with  
66 cell lysates to determine CASP8/CASP3/Gsdme activation by Western blot(Broz and

67 Monack, 2013). To quantify the amount of LPS delivered to macrophages,  $1 \times 10^6$  cells  
68 were transfected with a FITC-labelled LPS conjugate following the procedure described  
69 above. At the timepoint indicated, the media in each well was removed, cells were  
70 washed twice with 4mL of PBS, lysates were collected in 300uL of RIPA buffer by gently  
71 scraping, and the relative fluorescence intensity for each sample was measured with a  
72 fluorometric plate reader.

73

#### 74 Cell Death assays:

75 Cell death assays were conducted in 96-well format with BMDM or RAW cells  
76 plated at 40,000 cells per well. Media was collected at the indicated timepoints and the  
77 relative amount of LDH was determined using the CytoTox (Promega Cat# G1780)  
78 assay following manufacturer instructions. Alternatively, SYTOX Green (ThermoFisher  
79 Cat# S7020; 20nM) was included in Opti-MEM media added prior to treatment for  
80 inflammasome activation. Following treatment for inflammasome activation, SYTOX  
81 positive cells were enumerated using the IncuCyte S3 Live Cell Analysis Imaging  
82 System. Triton X-100 (0.05% final concentration) was added to a set of control wells  
83 with corresponding priming conditions to generate a total cell count and to calculate  
84 percent cell death ( $\% \text{ cell death} = ((\text{experimental count})/(\text{count from total lysis})) \times 100$ ).

85

#### 86 Protein analysis by Western blot:

87 Macrophages were plated in 6-well format at  $1 \times 10^6$  cells per well. Cell lysates  
88 were collected by removing the media in each well, washing with PBS, and lysing in a

89 low volume (50uL/well) of RIPA buffer containing protease inhibitors (Roche cOmplete  
90 inhibitor cocktail). Protein concentrations were determined by Bradford assay (Pierce  
91 Cat# 23236) according to manufacturer instructions and equal concentrations were  
92 loaded for separation by standard SDS-PAGE. For experiments characterizing released  
93 protein into the supernatant, a TCA precipitation protocol was used as previously  
94 described(Broz and Monack, 2013) and equal fractions were loaded for SDS-PAGE. For  
95 a complete list of the antibodies used for Western Blot in this publication, please refer to  
96 the Key Resource Table.

97

#### 98 Measurement of cytokine release by ELISA:

99 BMDM inflammasome activation for determining cytokine release were  
100 conducted in triplicate within a 96-well format and were plated at 40,000 cells per well  
101 as described above in the Cell Death assays section. Following inflammasome  
102 activation supernatants were collected at the indicated timepoints and stored at -20°C  
103 for future processing. The amount of IL-18 or IL-1 $\beta$  present in the supernatants was  
104 determined with commercially available ELISA kits by following manufacturer  
105 instructions (Invitrogen: IL-18 - Cat# BMS618-3TEN, IL-1 $\beta$  - Cat# 88-7013-88).

106

#### 107 Cell Lines Generated for this Manuscript:

108 RAW 264.7 KO cell lines (*Casp1/11* DKO, *Gsdmd* KO) were generated as  
109 previously described(Napier et al., 2016) and gRNAs are listed in the Key Resource  
110 Table. The cell line reconstituted with constitutive CASP11 expression was generated

111 on the *Casp1/11* DKO background with VSV pseudotyped retroviral constructs  
112 generated in 293T cells. The cDNA encoding CASP11 was isolated from BMDMs  
113 stimulated for 4hrs with LPS (100ng/mL) and cloned into pMSCV-IRES-GFP with  
114 XhoI/NotI. Transduced cells were isolated by FACS based on GFP expression and  
115 clonal populations were isolated. Untagged mouse NT-GSDMD PCR-amplified from  
116 Flag-GSDMD was Gibson cloned (NEB) into the pLenti CMVTRE3G Puro DEST  
117 inducible expression system using the EcoRV site. The cloned construct was introduced  
118 into *Gsdmd*-CRISPR/Cas9 KO RAW cells stably expressing the reverse tetracycline  
119 repressor-VP16 transactivator fusion protein pLenti CMV rtTA3G Blast using lentiviral  
120 delivery. Stable transductants were selected with puromycin and dilution plating was  
121 used to isolate the *Gsdmd*-CRISPR/Cas9 KO RAW Tet-On-NT-GSDMD clonal cell line.

122

### 123 Genome-wide CRISPR screen:

124 Our genome-wide CRISPR screen was conducted in the cell line that was  
125 created to constitutively express CASP11 (See above). Cells were stably transduced  
126 with lentiCas9-Blast (Addgene plasmid #52962) and selected with blasticidin to  
127 generate cells constitutively expressing Cas9. Lentiviral production of the Mouse  
128 CRISPR Knockout Pooled gRNA Library(Sanjana et al., 2014) (GeCKO V2; Addgene  
129 Cat# 1000000053) was generated by co-transfecting 150 million 293FT cells with a  
130 mixture of the plasmid library,  $\Delta$ VPR, VSV-G, pAdVantage packaging plasmids and  
131 EugeneHD. Lentiviral-containing supernatants were pooled from the total 293FT cell  
132 populations on day two and three following transfection, passed through a 0.45uM filter,



133 and stored at 4°C. This pooled lentiviral gRNA library was used to transduce a total of  
134 400 million constitutive CASP11-, Cas9-expressing cells at a MOI of 0.3 along with  
135 protamine sulfate (1ug/mL). Three days following transduction, cells containing the  
136 lentiviral gRNA constructs were selected with a five-day course of puromycin (5ug/mL).  
137 Each screen was conducted with a starting population of >100 million cells of the pooled  
138 gRNA library population to ensure sufficient knockout diversity by having an estimated  
139 >500-fold coverage of each gRNA in the library. For each screen two rounds of  
140 selection were conducted consisting of: 1) +/- IFN $\gamma$  priming 2) LPS transfection to  
141 activate CASP11 inflammasome 3) a recovery period. Briefly, cells were treated +/-  
142 IFN $\gamma$  (100 U/mL) for 16hrs in DMEM supplemented with 10%FBS and then the media  
143 was replaced with Opti-MEM just prior to LPS transfection. To trigger CASP11  
144 inflammasome activation, LPS (*E. coli* 0111:B4, InvivoGen) was complexed with  
145 FuGENE HD and transfected into the knockout library. Following transfection, Opti-  
146 MEM media containing LPS and FuGENE HD were removed and replaced with fresh  
147 DMEM 10% FBS once a substantial level of cell death was observed by eye. Cells  
148 surviving the CASP11 activation were allowed to expand prior to a second round of  
149 selection or prior to collection for isolating genomic DNA. An untreated starting  
150 population of the mutagenized library was used as the unselected reference for each  
151 screen. Total genomic DNA was isolated from the surviving cell populations as well as  
152 from the untreated starting population using QIAamp DNA MiniKits (Qiagen). Two  
153 rounds of PCR were used to amplify the gRNA sequences from each population and  
154 append barcodes for next-generation sequencing by MiSeq (Illumina). Finally, the

155 previously described MAGeCK algorithm was used to analyze our sequencing results  
156 and generate enrichment scores for each gRNA(Li et al., 2014).

157

158 OMV isolation:

159 E. coli DH5a was grown for 8 hours in LB broth at 200 rpm at 37°C. This starter  
160 culture was then back-diluted 1:1000 into 200 ml LB and grown shaking at 200 rpm  
161 overnight at 37°C. Bacteria were removed by pelleting at 5000 xg for 15 minutes, and  
162 the supernatant was passed through a 0.2 µm filter. OMVs were isolated by centrifuging  
163 the filtered supernatant in thick-wall polycarbonate tubes (Beckman Coulter Catalog No.  
164 355631) in a Type 70 Ti rotor in an Optima L-90K ultracentrifuge (Beckman Coulter) at  
165 149,000 xg at 4°C for 3 hours. Following centrifugation, the supernatant was removed  
166 and the resulting OMV pellet was resuspended in cell culture-grade 1x PBS pH 7.4  
167 (final concentration = 440x concentrated from culture broth). The resuspended OMVs  
168 were then passed through a 0.2 µm filter and stored at -80°C. This process was  
169 repeated to generate three batches of OMVs. Prior to addition to mammalian cells, the  
170 three batches were combined in a ratio of 1:1:1.

171

172 *Quantification and Statistical Analysis:*

173 Statistical calculations were conducted using GraphPad Prism software program.  
174 Two-way ANOVA statistical tests were conducted with multiple comparisons as  
175 indicated in each figure legend.

176

177 References:

- 178 BROZ, P. & MONACK, D. M. 2013. Measuring inflammasome activation in response to  
179 bacterial infection. *Methods Mol Biol*, 1040, 65-84.
- 180 LI, W., XU, H., XIAO, T., CONG, L., LOVE, M. I., ZHANG, F., IRIZARRY, R. A., LIU, J.  
181 S., BROWN, M. & LIU, X. S. 2014. MAGECK enables robust identification of  
182 essential genes from genome-scale CRISPR/Cas9 knockout screens. *Genome*  
183 *Biol*, 15, 554.
- 184 NAPIER, B. A., BRUBAKER, S. W., SWEENEY, T. E., MONETTE, P., ROTHMEIER, G.  
185 H., GERTSVOLF, N. A., PUSCHNIK, A., CARETTE, J. E., KHATRI, P. &  
186 MONACK, D. M. 2016. Complement pathway amplifies caspase-11-dependent  
187 cell death and endotoxin-induced sepsis severity. *J Exp Med*, 213, 2365-2382.
- 188 SANJANA, N. E., SHALEM, O. & ZHANG, F. 2014. Improved vectors and genome-wide  
189 libraries for CRISPR screening. *Nat Methods*, 11, 783-4.
- 190

## KEY RESOURCES TABLE

REAGENT or RESOURCE	SOURCE	IDENTIFIER
<b>Antibodies</b>		
Mouse monoclonal anti-beta-Actin	Sigma-Aldrich	Cat# A1978, RRID:AB_476692
Rabbit polyclonal anti-Caspase1 p10	Santa Cruz Biotechnology	Cat# sc-514, RRID:AB_2068895
Rabbit polyclonal anti-Cleaved Caspase3	Cell Signaling Technology	Cat# 9661, RRID:AB_2341188
Rabbit monoclonal anti-Cleaved Caspase8	Cell Signaling Technology	Cat# 8592, RRID:AB_10891784
Rat monoclonal anti-Caspase11 (clone 17D9)	Sigma-Aldrich	Cat# C1354, RRID:AB_258736
Rabbit polyclonal anti-GBP2	Proteintech	Cat# 11854-1-AP, RRID:AB_2109336
Rabbit monoclonal anti-GSDMD	Abcam	Cat# ab209845, RRID:AB_2783550
Rabbit monoclonal anti-GSDME	Abcam	Cat# ab215191, RRID:AB_2737000
Rabbit monoclonal anti-HMGB1	Abcam	Cat# ab79823, RRID:AB_1603373
Goat polyclonal anti-IL-1 $\beta$	R&D Systems	Cat# AF-401-NA RRID:AB_416684
Rabbit monoclonal anti-IL-18	Abcam	Cat# ab207323
Mouse monoclonal anti-NLRP3	AdipoGen	Cat# AG-20B-0014, RRID:AB_2490202
<b>Biological Samples</b>		
LPS VacciGrade Lipopolysaccharide from E. coli 0111:B4	InvivoGen	Cat# vac-3pelps
Cholera Toxin B Subunit in Low Salt	List Biological Labs	Cat# 104
<b>Chemicals, Peptides, and Recombinant Proteins</b>		
Recombinant IFN $\gamma$ Mouse Protein	ThermoFisher Scientific	Cat# PMC4031
Recombinant IFN $\beta$ 1 Mouse Protein	BioLegend	Cat# 581302
FuGENE HD transfection reagent	Promega	Cat# E2311
SYTOX Green Nucleic Acid Stain	ThermoFisher Scientific	Cat# S7020
Opti-MEM, no phenol red	ThermoFisher Scientific	Cat# 11058021
Nigericin	InvivoGen	Cat# tlr1-nig
ATP	InvivoGen	Cat# tlr1-atpl
(5Z)-7-Oxozeaenol (5z7)	Sigma-Aldrich	Cat# 499610
<b>Critical Commercial Assays</b>		
CytoTox 96 Non-Radioactive Cytotoxicity Assay	Promega	Cat# G1780
IL-1 $\beta$ Mouse Uncoated ELISA Kit	Invitrogen	Cat# 88-7013-88
IL-18 Mouse ELISA Kit	Invitrogen	Cat# BMS618-3TEN
<b>Experimental Models: Cell Lines</b>		
RAW 264.7	ATCC	Cat# TIB-71

Constitutive CASP11 expressing cell line: <i>Casp1, Casp11</i> CRISPR DKO +CASP11	This manuscript	
Experimental Models: Mouse Strains for BMDM isolation		
WT C57BL/6NJ	Jackson Labs	Stock No. 005304
<i>Ifngr1</i> <sup>-/-</sup>	Jackson Labs	Stock No. 003288
<i>Casp1</i> <sup>-/-</sup>	Gift of Vishva Dixit	
<i>Casp11</i> <sup>-/-</sup>	Gift of Vishva Dixit	
<i>Gsdmd</i> <sup>-/-</sup>	Gift of Vishva Dixit	
<i>Gsdme</i> <sup>-/-</sup>	Gift of Vishva Dixit	
<i>Gbp</i> <sup>chr3</sup> <sup>-/-</sup>	Gift of Petr Broz and Igor Brodsky	
Oligonucleotides		
gRNA Casp1: TGTCTCTAAAAAAGGGCCCC	Napier et al 2016	
gRNA Casp11: CTGAACGCAGTGACAAGCGT	Napier et al 2016	
gRNA Gsdmd: TCGTGGGGATGACCTGTTTG	GeCKO V2 library Sanjana et al. 2014	
Primer pair to clone constitutive Casp11: fwd- AAAACCTCGAGACTCTGTCAAGCTGTCTTACGGT rev- AAAAGCGGCCGCTCAGTTGCCAGGAAAGAGGTAGA AATAT	This manuscript	
Primer pair to clone NT-Gsdmd: fwd- CAGTGTGGTGAATTCTGCAGATGCCACCATGCCA TCGGCCTTTGAGAAAG rev- GCGGCCGCCACTGTGCTGGATCTAATCTGACAGGA GACTGAGCTGCTTTC	This manuscript	
Recombinant DNA		
Plasmid: MSCV-IRES-GFP	Addgene	Plasmid # 20672; RRID:Addgene_20672
Plasmid: pLenti CMVTRE3G Puro DEST	Addgene	Plasmid # 27565; RRID:Addgene_26429
Plasmid: pLenti CMV rTA3G Blast	Addgene	Plasmid # 26429; RRID:Addgene_26429
Plasmid: Flag-Gsdmd	Addgene	Plasmid # 80950; RRID:Addgene_80950
Plasmid: lentiCas9-Blast	Addgene	Plasmid #52962; RRID:Addgene_52962
Plasmid: Mouse CRISPR Knockout Pooled Library (GeCKO v2)	Addgene; Sanjana et al. 2014	Cat #1000000053
Software and Algorithms		
Prism8	GraphPad	
MAGeCK	Li et al. 2014	